HHS Public Access

Author manuscript

Mol Pharm. Author manuscript; available in PMC 2019 February 04.

Published in final edited form as:

Mol Pharm. 2018 November 05; 15(11): 4947–4962. doi:10.1021/acs.molpharmaceut.8b00592.

Preclinical Efficacy and Characterization of Candidate Vaccines for Treatment of Opioid Use Disorders Using Clinically Viable Carrier Proteins

Federico Baruffaldi[†,∇], **April Huseby Kelcher**[†,∇], **Megan Laudenbach**[†], **Valeria Gradinati**[†,‡], **Ajinkya Limkar**[§], **Michaela Roslawski**[§], **Angela Birnbaum**[§], **Andrew Lees**[‖], **Carla Hassler**[⊥], **Scott Runyon**[⊥], and **Marco Pravetoni**[*,†,#]

[†]Hennepin Healthcare Research Institute (HHRI, formerly Minneapolis Medical Research Foundation or MMRF), 701 Park Avenue, Minneapolis, Minnesota 55415, United States

[‡]Dipartimento di Chimica e Tecnologie Farmaceutiche, Socrates Program, Universitá degli Studi di Milano, Milan 20122, Italy

[§]University of Minnesota, Minneapolis, Minnesota 55455, United States

[‖]Fina Biosolutions, LLC, Rockville, Maryland 20850, United States

[⊥]RTI International, Research Triangle Park, North Carolina 27709-2194, United States

[#]Departments of Medicine and Pharmacology, Center for Immunology, University of Minnesota, Minneapolis, Minnesota 55455, United States

Abstract

Vaccines may offer a new treatment strategy for opioid use disorders and opioid-related overdoses. To speed translation, this study evaluates opioid conjugate vaccines containing components suitable for pharmaceutical manufacturing and compares analytical assays for conjugate characterization. Three oxycodone-based haptens (OXY) containing either PEGylated or tetraglycine [$(Gly)_4$] linkers were conjugated to a keyhole limpet hemocyanin (KLH) carrier protein via carbodiimide (EDAC) or maleimide chemistry. The EDAC-conjugated OXY$(Gly)_4$-KLH was most effective in reducing oxycodone distribution to the brain in mice. Vaccine efficacy was T cell-dependent. The lead OXY hapten was conjugated to the KLH, tetanus toxoid, diphtheria cross-reactive material (CRM), as well as the *E. coli*-expressed CRM (EcoCRM) and nontoxic tetanus toxin heavy chain fragment C (rTTHc) carrier proteins. All vaccines induced early hapten-specific B cell expansion and showed equivalent efficacy against oxycodone in mice.

[*]**Corresponding Author** prave001@umn.edu.

[∇]Author Contributions

F.B. and A.H.K. equally contributed to this work and are co-first authors

The authors declare the following competing financial interest(s): M.P. is the inventor of Cytokine Signaling Immunomodulators and Methods. Provisional Patent Application No. 62/334, 167 filed on May 10, 2016 and International Application No. PCT/US2017/031907 filed on May 10, 2017. A.L. is the Scientific Director at Fina BioSolutions, LLC. and owner. The other authors have no conflict of interest.

ASSOCIATED CONTENT

Supporting Information

The Supporting Information is available free of charge on the ACS Publications website at DOI: 10.1021/acs.molpharmaceut.8b00592.

Supplementary figures, methodology, and hapten synthesis details (PDF)

However, some hapten-protein conjugates were easier to characterize for molecular weight and size. Finally, heroin vaccines formulated with either EcoCRM or KLH were equally effective in reducing heroin-induced antinociception and distribution to the brain of heroin and its metabolites in mice. This study identifies vaccine candidates and vaccine components for further development

Graphical Abstract

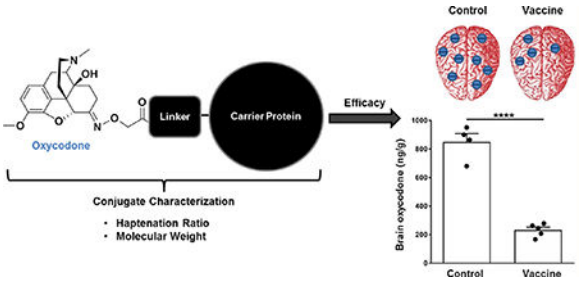

Keywords

conjugate vaccine; carrier protein; oxycodone; heroin; hapten; linkers

INTRODUCTION

Opioid use disorders (OUD) and opioid-induced fatal overdoses are a worldwide public health concern.[1] In recent years, countries such as the USA, Canada, and Europe have faced an increase in the incidence of OUD and fatal overdoses.[2–4] In the United States, OUD and overdoses involving heroin, prescription opioids, and synthetic opioids have reached epidemic proportions featuring over 250 000 hospitalizations and over 50 000 deaths in 2016.[5,6] The opioid epidemic is estimated to have cost the country more than $95 billion in work and healthcare-related expenses in 2016, and the national cost is estimated to have increased for 2017.[7] The current standard of care includes pharmacotherapy (e.g., opioid receptor agonists and antagonists), behavioral therapy, and counseling. However, only 1 in 5 opioid users access medications suggesting that more treatment options are needed.[5,8] The National Institute of Health leadership has recently advocated for development of new therapies for OUD and encouraged public-private partnerships as a viable path to speed up translation.[9]

Vaccines are being explored as a treatment strategy for OUD. Opioid vaccines are potentially safe and cost-effective immunotherapeutic interventions that elicit long-lasting opioid-specific antibodies, which decrease opioid distribution to the brain, reducing opioid self-administration, opioid-induced antinociception and locomotor activity, and opioid-induced respiratory depression and bradycardia, as well as fatal overdoses.[10–16] Preclinical proof of selectivity and efficacy has been shown against heroin and its metabolites, oxycodone, hydrocodone, and fentanyl in mouse, rat, and nonhuman primate studies.[11–14,17–25] These data support translation of vaccines as a novel treatment strategy for OUD, and warrant their testing in clinical trials to demonstrate clinical proof of concept for this approach. Although several clinical trials of nicotine and cocaine vaccines have been

conducted,[26–30] clinical evaluation of an opioid conjugate vaccine has been limited to a trial conducted in Iran, and for which scarce information is available.[31] One of the challenges in vaccine development is to use components and processes suitable for pharmaceutical manufacturing and regulatory approval. Continuous improvement of vaccine design, rational development of new vaccine components, and understanding the immunological mechanisms underlying effective immune responses against drugs of abuse will be important to speed translation of addiction vaccines.

A successful vaccination strategy against drugs of abuse involves optimal activation of the adaptive immune system to achieve effective drug-specific antibody levels required to antagonize clinically relevant drug doses.[28] The generation of effective drug-specific antibodies results from T cell-dependent B cell activation, which is achieved by conjugation of opioid-based haptens to larger immunogenic carriers that provide T cell signaling, and enhanced by formulation of conjugates in adjuvant or other immunomodulators.[28,32,33] It is well-established that hapten design affects antibody titer, affinity, and selectivity for the target drug.[14,24,25,34] Indeed, higher frequency of the precursor and early-activated hapten-specific B cell subsets has been shown to correlate with increased individual antibody titers and vaccine efficacy against nicotine and opioids.[22,35,36] Several studies have shown that vaccine efficacy against drugs of abuse is also affected by the choice of carrier, which is usually protein- or peptide-based or involves other novel platforms.[28,29] In fact, as the pre-immunization frequency of carrier-specific $CD4^+$ T cell lymphocytes correlates to vaccine efficacy against oxycodone, depletion of $CD4^+$ T cells prevents hapten-specific B cell activation, and efficacy of an oxycodone vaccine in mice,[35] highlighting the role for carrier proteins in providing T cell signaling.

This study focused on testing the effect of the hapten structure, conjugation chemistry, and carrier protein on the efficacy of vaccines against oxycodone and heroin, and it also compared analytical assays for characterization of these conjugate vaccines. First, we confirmed that haptens containing tetraglycine linkers conjugated to carrier proteins using carbodiimide chemistry generated the most effective vaccines against oxycodone in mice. Second, we demonstrated that generation of opioid-specific serum IgG antibodies is contingent upon integrity of T cell signaling in mice lacking a functional T cell receptor (TCR) or in wild-type (WT) mice immunized with oxycodone vaccine formulations lacking T cell epitopes. Third, we compared the efficacy of oxycodone conjugate vaccines containing keyhole limpet hemocyanin (KLH), subunit KLH (sKLH), tetanus toxoid (TT), cross-reactive material-197 (CRM_{197}), and two commercially available carriers that have been expressed at high levels as soluble, intracellular proteins in *E. coli*, the *E. coli*-expressed CRM (EcoCRM)[37] and the nontoxic tetanus toxin heavy chain fragment C (rTTHc).[38] Fourth, we compared analytical assays for characterization of opioid-protein conjugates and found that matrix-assisted laser desorption/ionization-time of flight (MALDI-TOF) and dynamic light scattering (DLS) were optimal techniques to qualify conjugates. Fifth, we compared the efficacy of heroin vaccines containing either EcoCRM or sKLH. We concluded that EcoCRM, rTTHc, CRM_{197}, KLH, and sKLH were viable carrier alternatives for the development of vaccines against OUD and other drugs of abuse. The vaccines and vaccine components developed herein are considered for further development.

EXPERIMENTAL SECTION

Drugs and Reagents.

Oxycodone and heroin were obtained through the NIDA Drug Supply Program and Sigma (St. Louis, MO), and doses are expressed as the weight of the base. Alum (Alhydrogel 85, Brenntag Biosector, Frederikssund, Denmark) was used according to the manufacturer instructions.

Synthesis of Oxycodone- and Morphine-Based Haptens.

OXY(Gly)$_4$OH Hapten.—The oxycodone-based hapten modified at the C6 position of the morphinan structure (OXY) with a tetraglycine $(Gly)_4$ linker was synthesized as previously described.[20,39]

OXY(PEG)$_3$OH Hapten.—The oxycodone-based hapten containing a polyethylene glycol $(PEG)_3$ linker was synthesized as described below and in more detail in the Supporting Information (S1).

Chemistry General.

All standard reagents were commercially available. Intermediates were purified by column chromatography on a Teledyne ISCO Rf chromatography unit unless otherwise indicated. The purity of the intermediates and final compounds was determined using an Agilent-Varian HPLC system equipped with Prostar 210 dual pumps, a Prostar 335 diode UV detector, and a SEDEX75 (SEDERE, Olivet, France) ELSD detector, and an analytical Synergy Hydro RP80A C18 (4 μm 250 mm × 4.60 mm; Phenomenex) column with a linear gradient of 5–95% solvent B over 20 min at a flow rate of 1 mL/min was used. Absorbance was monitored at 220 nm. The HPLC solvent system was binary with solvent A as water containing 0.1% trifluoroacetic acid (TFA) and solvent B as acetonitrile containing 5% water and 0.1% TFA. The molecular ion of the intermediates and final compounds as determined using a PE Sciex API 150 EX LC/MS system from PerkinElmer (San Jose, California). Reactions were monitored by thin-layer chromatography (TLC) carried out on precoated 60 Å 250 mm silica gel TLC plates with the F-254 indicator visualized under UV light. ESI-HRMS spectra were obtained on a Waters-SYNAPT-G2 mass spectrometer. ^{1}H NMR spectra were recorded at 300 MHz on a Bruker Avance 300 Spectrospin instrument and are reported as follows: chemical shift δ in ppm (multiplicity, coupling constant (Hz), and integration). The following abbreviations were used to explain multiplicities: s = singlet, d = doublet, t = triplet, q = quartet, quin = quintet, m = multiplet, br = broad, and dd = doublet of doublets.

Methyl 1-(9H-Fluoren-9-yl)-3-oxo-2,7,10,13-tetraoxa-4-azapentadecan-15-oate, Fmoc-HN-Peg$_3$-O–CH$_2$CO$_2$Me.—To a solution of methyl {2-[2-(2-aminoethoxy)ethoxy]ethoxy}acetate (**H$_2$N-Peg$_3$-O–CH$_2$CO$_2$H**, 500 g, 1.16 mmol) in methanol/THF (1:5, 12 mL) was added pyBOP (905 mg, 1.74 mmol), DIEA (808 uL, 4.64 mmol), and DMAP (14 mg, 0.12 mmol). The reaction mixture was stirred at room temperature (rt) for 12 h. The mixture was concentrated in vacuo to provide methyl 1-(*9H*-fluoren-9-yl)-3-oxo-2,7,10,13-tetraoxa-4-azapentadecan-15-oate (**Fmoc-HN-Peg$_3$-O–**

CH_2CO_2Me, 514 mg, quant.) as a crude mixture. ^{1}H NMR (300 MHz, DMSO-d_6, δ ppm): 3.24–3.59 (m, 15 H), 3.63 (s, 3 H), 4.12 (s, 1 H), 4.18–4.24 (m, 1 H), 4.28 (s, 1 H), 4.36 (s, 1 H), 7.25–7.46 (m, 5 H), 7.59 (d, J = 8.29 Hz, 1 H), 7.69 (d, J = 6.97 Hz, 1 H), 7.82–7.93 (m, 2 H). ESI-MS (m/z): $(M+Na)^+$ calcd for $C_{24}H_{29}NO_7$, 443.5; found, 466.7.

Methyl {2-[2-(2-Aminoethoxy)ethoxy]ethoxy}acetate, H_2N-Peg_3-O-CH_2CO_2Me.—To a solution of crude methyl 1-(*9H*-fluoren-9-yl)-3-oxo-2,7,10,13-tetraoxa-4-azapentadecan-15-oate (**Fmoc-HN-Peg_3-O–CH_2CO_2Me**) in methanol (15 mL) was added piperidine (3 mL), and the reaction mixture was stirred at rt for 6 h. The reaction mixture was concentrated and dried in vacuo to provide methyl {2-[2-(2-aminoethoxy)-ethoxy]ethoxy}acetate (**H_2N-Peg_3-O–CH_2CO_2Me**) as a crude mixture. ESI-MS (m/z): $(M+H)^+$ calcd for $C_9H_{19}NO_5$, 221.2; found, 222.2.

({[(6E)-14-Hydroxy-3-methoxy-17-methyl-4,5-epoxymorphinan-6-ylidene]amino}oxy)acetic Acid, Oxy-Glyoxime–OH.—To a solution of 14-hydroxy-3-methoxy-17-methyl-4,5-epoxymorphinan-6-one hydrochloride salt (oxycodone HCl, 2.0 g, 6.34 mmol) in MeOH (10 mL) was added 1 M NaOH (6.6 mL, 1.05 equiv). The reaction mixture was stirred for 15 min, concentrated, and dried in vacuo for 2 h. The residue was redissolved in anhydrous MeOH (200 mL) and carboxylmethoxylamine (1.04 mg, 9.5 mmol), and pyridine (1.52 mL, 3.0 equiv) was added. The mixture was stirred at reflux temperature for 16 h, cooled to rt, and concentrated in vacuo. The residue was redissolved in acetone (10 mL) and precipitated with ether (120 mL). The precipitate was collected, reprecipitated, and dried in vacuo to provide ({[(*6E*)-14-hydroxy-3-methoxy-17-methyl-4,5-epoxymorphinan-6-ylidene]amino}oxy)acetic acid (**Oxy-Glyoxime–OH**) as a white powder (2.6 g, 70% yield). ^{1}H NMR (300 MHz, DMSO-d_6, δ ppm): 1.08–1.25 (m, 2 H), 1.35–1.62 (m, 3 H), 1.81 (d, J = 9.23 Hz, 1 H), 2.30 (br. s., 2 H), 2.41–2.46 (m, 3 H), 2.63 (br. s., 2 H), 3.05 (br. s., 2 H), 3.14–3.23 (m, 1 H), 3.71–3.80 (m, 3 H), 4.55 (s, 2 H), 4.94 (br. s., 1 H), 6.69 (d, J = 7.72 Hz, 1 H), 6.81 (d, J = 8.10 Hz, 1 H). ESI-MS (m/z): $(M+H)^+$ calcd for $C_{20}H_{24}N_2O_6$, 388.4; found, 389.7. HPLC (Synergy Hydro, 20 min) t_R = 11.32 min (>99%).

Methyl 14-({[(6E)-14-Hydroxy-3-methoxy-17-methyl-4,5-epoxymorphinan-6-ylidene]amino}oxy)-13-oxo-3,6,9-trioxa-12-azatetradecan-1-oate, Oxy-Glyoxime-HN-Peg_3-O-CH_2CO_2Me.—To a clear solution of ({[(6E)-14-hydroxy-3methoxy-17-methyl-4,5-epoxymorphinan-6-ylidene]amino}oxy)acetic acid (**Oxy-Glyoxime–OH**, 186 mg, 0.48 mmol) in DMF (20 mL) was added pyBOP (328 mg, 0.63 mmol), methyl {2-[2-(2-aminoethoxy)ethoxy]ethoxy}acetate (**H_2N-Peg_3-O–CH_2CO_2Me**) (128 mg, 0.58 mmol), and then DIEA (418 μL, 2.4 mmol). The reaction mixture was stirred at rt for 6 h under nitrogen atmosphere and then concentrated to dryness in vacuo. The residue was purified by column chromatography [20 g SiO_2, eluent DCM 100% to 50% CMA 80 (Chloroform/MeOH/NH_4OH 80/19.8/0.2)] to provide methyl 14-({[(*6E*)-14-hydroxy-3-methoxy-17-methyl-4,5-epoxymorphinan-6-ylidene]amino}oxy)-13-oxo-3,6,9-trioxa-12-azatetradecan-1-oate (**Oxy-Glyoxime-HN-Peg_3-O-CH_2CO_2Me**) as a white powder (94 mg. 32%). ESI-MS (m/z): $(M+H)^+$ calcd for $C_{29}H_{41}N_3O_{10}$ 591.7; found, 592.2. HPLC (Synergy Hydro, 20 min) t_R = 12.37 min (95%).

Lithium 14-({[(6E)-14-Hydroxy-3-methoxy-17-methyl-4,5-epoxymorphinan-6-ylidene]amino}oxy)-13-oxo-3,6,9-trioxa-12-azatetradecan-1-oate, Oxy-Glyoxime-HN-Peg$_3$-O–CH$_2$CO$_2$Li.—To a solution of methyl 14-({[(*6E*)-14-hydroxy-3-methoxy-17-methyl-4,5-epoxymorphinan-6-ylidene]amino}-oxy)-13-oxo-3,6,9-trioxa-12-azatetradecan-1-oate (**Oxy-Glyoxime-HN-Peg$_3$-O-CH$_2$CO$_2$Me**, 32 mg, 0.054 mmol) in MeOH/THF (1:1, 4 mL) was added H_2O (0.5 mL) and then LiOH (1.3 mg, 0.054 mmol). The reaction mixture was stirred at rt for 6 h, concentrated to dryness, and dried in vacuo. The residue was redissolved in minimal MeOH and precipitated with Et_2O to provide lithium14-({[(*6E*)-14-hydroxy-3-methoxy-17-methyl-4,5-epoxymorphinan-6-ylidene]amino}oxy)-13-oxo-3,6,9-trioxa-12-azatetradecan-1-oate (**Oxy-glyoxime-HN-Peg$_3$-O–CH$_2$CO$_2$Li**) as a white powder (12 mg, 38%). ^{1}H NMR (300 MHz, DMSO-d_6, δ ppm): 1.14–1.27 (m, 1 H), 1.29–1.59 (m, 3 H), 1.99–2.26 (m, 3 H), 2.31 (s, 4 H), 2.34–2.47 (m, 2 H), 2.79 (d, J = 6.03 Hz, 1 H), 3.13 (d, J = 18.65 Hz, 1 H), 3.19–3.29 (m, 3 H), 3.37–3.58 (m, 9 H), 3.69–3.80 (m, 4 H), 4.44 (s, 2 H), 4.79–4.89 (m, 2 H), 6.60–6.70 (m, 1 H), 6.72–6.80 (m, 1 H), 7.83 (t, J = 5.56 Hz, 1 H). ESI-MS (m/z): $(M+H)^+$ calcd for $C_{28}H_{38}LiN_3O_{10}$, 583.6; found, 584.9. HPLC (Synergy Hydro, 20 min) t_R = 11.31 min (95%).

OXY(Gly)$_4$-SH Hapten.—An alternative OXY(Gly)$_4$ hapten containing a terminal thiol (SH) group on the C-term of the tetraglycine linker was synthesized as described below and in more detail in the Supporting Information (S2).

N-[({[(5α,6E)-14-Hydroxy-3-methoxy-17-methyl-4,5-epoxymorphinan-6-ylidene]amino}oxy)acetyl]glycylglycylglycylN-(2-sulfanylethyl)glycinamide (Oxy-Glyoxime-Gly$_4$-NH-(CH$_2$)$_2$SH).—To a clear solution of lithium *N*-[({[(*6E*)-14-hydroxy-3-methoxy-17-methyl-4,5-epoxymorphinan-6-ylidene]amino}oxy)acetyl]glycylglycyl-*N*-(carboxylatomethyl)-glycinamide (**Oxy-Glyoxime-Gly$_4$-OLi**, 200 mg, 0.32 mmol) in DMF (30 mL) was added BOP (284 mg, 0.643 mmol), 2-(tritylthio)ethanamine (123 mg, 0.386 mmol), and then diisopropylethylamine (280 μL, 1.61 mmol). The reaction mixture was stirred at rt for 16 h under nitrogen atmosphere and then dried in vacuo. The residue was purified by column chromatography [24 g SiO_2, eluent 0 to 40% CMA 80 (chloroform/MeOH/NH_4OH 80/19.8/0.2) in DCM] to provide *N*-[({[(*5α,6E*)-14-hydroxy-3-methoxy-17-methyl-4,5-epoxymorphinan-6-ylidene]amino}oxy)acetyl]-glycylglycylglycyl-*N*-[2-(tritylsulfanyl)ethyl]glycinamide (**OxyGlyoxime-Gly$_4$-NH-(CH$_2$)$_2$STrtl**) as a yellow powder (192 mg. 65%). To a solution of this material in DCM/MeOH (10 mL/4 mL) was added TFA (6 mL) and triethylsilane (0.3 mL), and the solution was stirred at rt for 1 h. The mixture was concentrated to dryness and purified by column chromatography [12 g SiO_2, eluent 0–40% CMA 80 (chloroform/MeOH/NH_4OH 80/19.8/0.2) in DCM] to provide **Oxy-Glyoxime-Gly$_4$-NH-(CH$_2$)$_2$SH** (91 mg, 64%) as a white powder. ^{1}H NMR (300 MHz, DMSO-d_6, δ ppm): 1.12–1.31 (m, 1 H), 1.39–1.69 (m, 2 H), 2.25–2.43 (m, 2 H), 2.55–3.03 (m, 10 H), 3.09–3.27 (m, 4 H), 3.56–4.03 (m, 12 H), 4.45–4.63 (m, 2 H), 5.01 (br. s., 1 H), 6.62–6.87 (m, 2 H), 7.79–7.97 (m, 2 H), 8.06–8.28 (m, 3 H). ESI-MS (m/z): $(M+H)^+$ calcd for $C_{30}H_{41}N_7O_9S$, 675.76; found, 676.6. HPLC (Synergy Hydro, 20 min) t_R = 10.96 min (>95%).

(Oxy-Glyoxime-Gly$_4$-NH-(CH$_2$)$_2$S)$_2$.—To a solution of *Oxy-Glyoxime-Gly$_4$-NH-(CH$_2$)$_2$SH* (87 mg, 0.129 mmol) in water/acetonitrile/methanol (40 mL, ratio 2/1/1) was added pH 8.5 NH_4OAc buffer solution (2.5 mL), and the reaction mixture was saturated with nitrogen. Potassium ferricyanide (125 mg, 0.380 mmol) was added, and the reaction mixture was stirred at rt for 16 h. The solution was acidified to pH 3.5 with glacial acetic acid, stirred over Amberlite IRA-68 resin for 20 min, and then filtered. The filtrate was concentrated to dryness and purified by column chromatography [130 g C18, eluent 0–100% MeOH in water] to provide (**Oxy-GlyoximeGly$_4$-NH-(CH$_2$)$_2$S)$_2$** (79 mg, 91%) as a white solid. ^{1}H NMR (700 MHz, DMSO-d_6, δ ppm): 1.47 (d, J = 5.72 Hz, 6 H) 2.33–2.44 (m, 3 H) 2.57–2.86 (m, 14 H) 3.29–3.46 (m, 11 H) 3.61–3.82 (m, 26 H) 4.52 (br. s., 4 H) 5.11 (br. s., 2 H) 6.68–6.78 (m, 1 H) 6.83–6.90 (m, 1 H) 7.09–7.15 (m, 1 H) 7.19–7.38 (m, 4 H) 7.65–7.77 (m, 1 H) 7.89–7.97 (m, 1 H) 8.01–8.09 (m, 1 H) 8.15 (br. s., 4 H). ESI-HRMS (*m/z*): calcd for $C_{60}H_{80}N_{14}O_{18}S$, 1349.50; found, 1349.53 $(M)^+$, 675.27 $(M)^{2+}$. HPLC (Synergy Hydro, 20 min) t_R = 11.59 min (>95%).

M(Gly)$_4$OH Hapten.—The design of this morphine-based hapten is analogous to the OXY(Gly)$_4$OH hapten, and the M(Gly)$_4$ Li^{2+} salt hapten was synthesized as previously described.[20] Immunization with the M(Gly)$_4$OH hapten conjugated to KLH and sKLH elicits antibodies effective and selective for heroin and its metabolites 6-acetylmorphine (6AM) and morphine.[15]

Conjugation to Carrier Proteins and Polymers.

Carbodiimide Coupling Chemistry.—OXY(Gly)$_4$, OXY(PEG)$_3$ haptens (5.2 mM, final concentration), and *N*-ethyl-*N*′-(3 dimethylaminopropyl) carbodiimide hydrochloride (EDAC, Sigma-Aldrich, St. Louis, MO) cross-linker (52 mM, final concentration) were dissolved in 0.1 M MES buffer pH 4.5. After stirring for 10 min, native KLH (mcKLH #7653, Thermo Fisher, Rockford, IL, Figures 1, 2, 3, and 5), subunit KLH (sKLH, GMP grade, Biosyn, Carlsbad, CA, Figures 3E,F, and 7), TT and CRM$_{197}$ (Walvax Biotechnology Co., Kunming, China), and EcoCRM and rTTHc proteins (Fina Biosolutions, LLC., Rockville, MD) were added at a final concentration of 2.8 mg/mL. Conjugation conditions were optimized using the model protein BSA as previously described.[39] Reactions were stirred for 3 h at rt. After 3 h, the MES buffer was exchanged with PBS buffer pH 7.2 using an Amicon filter unit (Merk Millipore, Burlington, MA), and the conjugate was resuspended to a final concentration of 2.5 mg/mL (KLH and sKLH) and 2.33 mg/mL (TT, CRM$_{197}$, rTTHc, and EcoCRM). Conjugates were stored at +4 °C. With the exception of OXY-KLH and OXY-sKLH, all of the other OXY-containing conjugates received 250 mM sucrose as a stabilizing agent within the reaction environment as well as in the final storage solution. For use as a coating antigen in ELISA, OXY was conjugated to chicken ovalbumin (OVA) (Sigma-Aldrich, St. Louis, MO). For magnetic enrichment of hapten-specific B cells paired to flow cytometry analysis, OXY was conjugated to red-phycoerytrin (PE) (Prozyme, Hayward, CA), as described.[22,35]

The OXY(Gly)$_4$OH hapten was conjugated to aminodextran (500 kDa) and amino-ficoll (400 kDa) functionalized with 100 primary amines (Fina Biosolutions, LLC., Rockville, MD). The OXY(Gly)$_4$OH hapten was activated with EDAC (52 mM) and 128 mM sulfo-*N*-

hydroxysuccinimide (sulfo-NHS, Thermo Fisher Scientific, Waltham, MA) in MES buffer pH 5.0 with 10% DMSO. Upon conversion to the NHS ester, the pH of the solution containing the activated hapten was increased to 7.0 using sodium hydroxide. Conjugations proceeded for 2 h at rt, and then conjugates were purified as described above.

The $M(Gly)_4OH$ hapten was conjugated to sKLH and EcoCRM using EDAC. $M(Gly)_4OH$ hapten was first conjugated to sKLH by dissolving 5.2 mM of hapten and 208 mM of EDAC in MES pH 4.5, as described in the section above. Instead, $M(Gly)_4OH$ was conjugated to EcoCRM by dissolving 5.2 mM of hapten and 104 mM of EDAC in MES pH 6.0 in the presence of 250 mM sucrose. $M(Gly)_4OH$ was also conjugated to OVA for ELISA. Reactions were stirred for 3 h at rt. After 3 h, the MES buffer was exchanged with the PBS buffer pH 7.2, as described above.

Maleimide Coupling Chemistry.—The thiol containing $OXY(Gly)_4$-SH hapten was conjugated to maleimide-activated KLH as described before for other haptens with minor modifications.[14,40] KLH (Thermo Scientific, Waltham, MA) (10 mg/mL in PBS pH 7.2) was activated with sulfosuccinimidyl 4-[*N*-maleimidomethyl] cyclohexane-1-carboxylate (Sulfo-SMCC, Thermo Scientific, Waltham, MA) at a ratio of 80:1 Sulfo-SMCC to KLH for 2 h at rt. The maleimide-activated protein was desalted using an Amicon filter unit (Merk Millipore, Burlington, MA). The hapten was dissolved in 715 μL of PBS pH 7.2 containing 1 mM ethylenediaminetetraacetic acid EDTA and 50 mM (tris(2-carboxyethyl)phosphine) TCEP (Sigma-Aldrich, St. Louis, MO) and added to the KLH solution; the conjugation proceeded for 4 h at rt. After 4 h, conjugates were filtered (Amicon) and stored in PBS pH 7.2 at 4 °C.

Characterization of Conjugates.

MALDI-TOF.—The molecular weight and the haptenation ratio (the hapten:carrier protein molar ratio) were calculated [((MW hapten + carrier protein) – MW carrier protein)/MW of hapten] for each conjugate using an Applied Biosystems/MDS SCIEX 5800 MALDI TOF/TOF analyzer (Foster City, CA) and TOF/TOF 5800 System Software (SCIEX, Concord, Ontario, Canada). The instrument operated in a high-mass linear mode. Samples were desalted on a ZipTip C4 (Merk Millipore, Burlington, MA) prior to analysis. Bovine serum albumin (BSA) was used to calibrate the instrument.

DLS.—Conjugates were assessed using a Zetasizer Nano S90 (SN MAL1165913, Malvern Instruments Ltd., Malvern, United Kingdom) instrument equipped with a 633 nm laser and 10–50 mW output power range. Measurements were performed with 75 μL of sample solution in 0.01 M PBS pH 7.2 at a constant temperature of 25 °C using a 1 mL cuvette (Sarstedt AG & Co. REF 67.754). Data were acquired with a 173-degree backscatter and analyzed using Zetasizer software 7.12. Raw data were exported to Microsoft Excel and statistically analyzed with Prism.

Size Exclusion-High-Performance Liquid Chromatography (SEC-HPLC).—Samples were analyzed on a Shimadzu Prominence LC-20AD dual pump system with a SPD-20A UV/vis spectrophotometer detector (Shimadzu Scientific Instruments Inc.,

Columbia, MD), and using a GE Healthcare Superose 6 Increase column (10 mm× 300 mm, 8.6 μm, 40 000 kDa exclusion limit, GE Healthcare Bio-Sciences, Marlborough, MA). The analysis was performed at 280 and 230 nm wavelengths using a 0.5 mL/min flow rate and 10 μL injection volume. PBS solution at pH 7.0 mobile phase was selected due to compatibility with solutions contained in samples of interest without hindering separation, resolution, and elution of the molecular weight standards (BioRad #151–1901). Several injections of exclusively mobile phase were run throughout the batch to ensure that there was no peak carryover and/or peak from the mobile phase contributing to the baseline. Run time was determined based on the length of time it took for the size standards to elute (average ~40 min). In instances where an aggregate peak eluted into the next sample injection, run time was extended to include all sample peaks, and size standards were re-analyzed to verify column efficiency.

Sodium Dodecyl Sulfate-Polyacrylamide Gel Electrophoresis (SDS-PAGE).— Samples were prepared as follows: 4 μL of loading buffer containing 1X β-mercaptoethanol (Bio-Rad, #1610710) and 9X Laemmli sample buffer (Bio-Rad, #1610747) were added to 12 μL of diluted sample (1 μg). The mixture was incubated for 10 min at rt and then heated at 95 °C for 5 min in a water bath. Samples were loaded on a precast, gradient, 3–8% polyacrylamide gel (Bio-Rad, Criterion XT Precast Gel, #3450129) using a running buffer (1X 20X-XT-Tricine (Bio-Rad, #1610790); 19X dH_2O) according to the manufacturer's instructions. SDS PAGE was run at 100 V constant voltage for 45 min and then 120 V for 25 min. The gel was stained with blue Coomassie Brilliant Blue for 1 h, and the gel image was acquired using the Bio-Rad, ChemiDoc-Touch Imaging system.

Animal Studies.

Ethics Statement.—All studies received approval from the HHRI (formerly MMRF) Institutional Animal Care and Use Committee. All animals were euthanized using AALAC-approved CO_2 inhalation chambers, and efforts were made to minimize suffering and discomfort.

Animals.—The 5-week-old male BALB/c (Harlan Laboratories, Madison, WI), C57BL/6, and TCR$\alpha^{-/-}$ (C57BL/6) (The Jackson Laboratory, Bar Harbor, ME) mice were group housed with a 12/12 h light/dark cycle and provided with mouse chow and water *ad libitum*.

Experimental Design.

In Vivo Screening of Vaccine Efficacy against Oxycodone and Heroin.—Mice were immunized with vaccine candidates or unconjugated carrier proteins as the control according to the immunization groups detailed below. A week after the last immunization, mice were assessed for opioid-specific serum IgG antibody titers and then challenged with opioid doses to test vaccine efficacy in retaining opioid in serum and reducing either opioid distribution to the brain or opioid-induced behavior. Mice immunized with oxycodone vaccines were challenged with 2.25 mg/kg oxycodone sc, and 30 min postchallenge mice were euthanized, and their trunk blood and brain were collected for analysis of oxycodone concentration by gas chromatography mass spectrometry (GC/MS), as previously described.[39] Mice immunized with heroin vaccines were challenged with 1 mg/kg heroin sc, and at 30

min postdrug challenge, mice were tested for heroin-induced antinociception on a hot plate at 54 °C, and then their trunk blood and brain were collected for measurement of heroin and its metabolites 6-AM and morphine by liquid chromatography mass spectrometry (LC/MS), as previously described.[15] The reported drug concentrations represent the total drug (protein- or antibody-bound as well as free) in each sample.

Immunization Groups.

1. Test effect of hapten and linker chemistry on vaccine efficacy against oxycodone. Mice were intramuscularly (IM) immunized on days 0, 14 and 28 with 75 μg of conjugate formulated with 250 μg of alum adjuvant.
2. Test effect of T cell signaling on generation of oxycodone-specific antibodies. C57BL/6 background WT and TCR$\alpha^{-/-}$ mice were subcutaneously (sc) immunized on days 0, 14, and 28 with 75 μg of conjugate formulated with 1 mg of alum adjuvant.
3. Test effect of carrier proteins on vaccine efficacy against oxycodone. Mice were sc immunized on days 0, 14 and 28 with 100 μg of conjugate formulated with 1 mg of alum adjuvant.
4. Test effect of carrier proteins on early expansion of B cells specific for the oxycodone-based hapten. Mice were IM immunized on day 0 with 100 μg of conjugate formulated with 250 μg of alum adjuvant. Spleen and lymph nodes were collected on day 7 post-immunization.
5. Test effect of carrier proteins on vaccine efficacy against heroin. Mice were IM immunized on days 0, 14, and 28 with 50 μg of conjugate formulated with 300 μg of alum adjuvant.

Analysis of Hapten-Specific B cell Population Subsets by Antigen-Based Magnetic Enrichment Paired with Flow Cytometry.

Analysis of hapten-specific B cells was conducted by antigen-based magnetic enrichment paired with flow cytometry, as previously described.[22,35] Lymph nodes and the spleen from individual mice were reduced to a single cell suspension by manual homogenization and subsequent enzymatic digestion with collagenase D (Roche, Indianapolis, IN). Samples were incubated with the control PE-AF647 decoy reagent followed by OXY-PE and then magnetically enriched by means of anti-PE-conjugated magnetic MicroBeads and magnetic columns (Miltenyi Biotec Inc., Auburn, CA). After enrichment, samples were stained for cell surface markers using the following fluorochrome-conjugated antibodies: antiGL7 (FITC, BD Pharmigen, San Diego, CA), anti-B220 (PE-Cy7 eBioscience, San Diego, CA), anti-IgM (APC, eBioscience), anti-CD38 (AF700, eBioscience), anti-IgD (ef450, eBioscience), anti-CD90.2 (APC-ef780, eBioscience), anti-Gr1 (APC-ef780, eBioscience), anti-CD11c (APC-ef780, eBioscience), and anti-F4/80 (APC-ef780, eBioscience). Samples were fixed, permeabilized (BD Bioscience cytoperm buffer), and stained with anti-IgG (H&L, Pacific Orange, Invitrogen, Carlsbad, CA). Samples were analyzed using a BD LSR II FORTESSA (BD Bioscience, San Jose, CA). The gating strategy was previously described in detail.[22,35,41] After identification of singlets, live lymphocytes were identified by side and

forward scatter, which excluded dead/dying cells and larger phagocytic cells. Next, B cells were identified as cells that express immunoglobulin (IgG^+) but not the following non-B cell markers: CD90.2 (T cells), Gr-1 (neutrophils), CD11.c (dendritic cells), and F4/80 (macrophages). To differentiate between OXY-binding B cells from PE-binding B cells, B cells were further gated as PE^+ (OXY-specific B cells) or AF647-PE^+ (PE-specific B cells). The OXY-specific B cell population was further identified as $B220^{neg}$ and IgG^{high} antibody secreting cells (plasma cells), $B220^{high}$ $CD38^{high}$ naïve/memory B cells, or $GL7^{high}$ germinal center (GC) B cells. $CD38^{high}$ cells were further identified as IgM^{high} B cells or IgM^{neg} IgD^{neg} switched memory B cells. Hapten-specific B cells were expressed as the percentage (%) of the total lymphocyte population after magnetic enrichment. All data were analyzed using FlowJo analysis software (Tree Star, Ashland, OR).

Oxycodone- and Heroin-Specific Serum IgG Antibody Analysis.

At completion of the immunization protocol and prior to the opioid challenge, mice were bled by facial vein puncture to obtain blood samples for antibody analysis. Oxycodone- and heroin-specific serum IgG antibody titers were determined by an indirect ELISA. Antibody titers were assessed as follows: 96-well plates were coated with 5 ng/well of either OXY-OVA or M-OVA conjugates or unconjugated OVA control in carbonate buffer at pH 9.6 and blocked with 1% gelatin. Primary antibodies were incubated with goat anti-mouse IgG antibodies conjugated to horseradish peroxidase to measure oxycodone- or heroin-specific serum IgG titers, as described previously.[20,39] When relevant, antibody affinity for oxycodone was determined by competitive binding ELISA to calculate IC_{50} values, as previously described with minor modifications.[39] Briefly, 96well plates were coated and blocked as above. Then, competitor dilutions of oxycodone were added at concentrations ranging from 0.01 to 1×10^{-13} M. Primary antibodies were added at a concentration that produced approximately 0.8 OD value by the ELISA titer assay. Secondary antibodies and substrate (SIGMAFAST OPD, Sigma-Aldrich, St. Louis, MO) were the same for all of the ELISA protocols.

Statistical Analysis.

Normality, skewness and kurtosis, and variance were assessed in each data set, and the corresponding statistical tests used are detailed in each figure legend. Data were analyzed using Prism 7.2 (GraphPad, San Diego, CA).

RESULTS

Hapten Design and Conjugation Chemistry Affect Vaccine Efficacy against Oxycodone.

Vaccine formulations containing three distinct oxycodone-based haptens and two different conjugation methods were evaluated for their efficacy in reducing oxycodone distribution to the brain in mice. First, we evaluated oxycodone-based haptens containing tetraglycine and PEG-based linkers (Figure 1A). The well-characterized $OXY(Gly)_4$ hapten[14] was first compared to the new $OXY\text{-}(PEG)_3$ of analogous length and attachment at the same C6 position. Then, the $OXY(Gly)_4$ hapten was compared to an equivalent $OXY(Gly)_4$ hapten with a modified C-term presenting a thiol group (–SH) for maleimide chemistry. All three haptens were conjugated to native KLH, formulated in alum adjuvant, and tested in BALB/c

mice immunized on days 0, 14, and 28. On day 35 post-immunization, mice were sc challenged with 2.25 mg/kg oxycodone, and then blood and brain were collected 30 min post-drug administration to evaluate vaccine efficacy in retaining oxycodone in serum and reducing oxycodone distribution to the brain. Immunization with $OXY(Gly)_4$-KLH produced higher IgG titers of $140 \pm 15 \times 10^3$ (mean ± SEM, Figure 1B, $p \leq 0.0001$) and significantly increased serum oxycodone concentrations compared to the KLH, $OXY(PEG)_3$-KLH, or $OXY(Gly)_4$-S-KLH immunization groups ($p \leq 0.0001$, Figure 1C). Higher serum oxycodone concentrations indicate that oxycodone is bound to antibodies, which decrease the amount of free (unbound) oxycodone that can cross the blood brain barrier. We have previously shown that immunization with $OXY(Gly)_4$-KLH increased bound and reduced unbound (free) oxycodone in rat serum.[14,39] Consequently, in this study, immunization with $OXY(Gly)_4$-KLH showed greater efficacy in reducing distribution of oxycodone to the brain compared to mice immunized with KLH, $OXY(PEG)_3$-KLH, or $OXY(Gly)_4$-S-KLH ($p \leq 0.0001$, Figure 1D). Because of its efficacy in vivo, the $OXY(Gly)_4$ hapten containing a C-terminal carboxyl group was selected for further development in subsequent studies.

Vaccine Efficacy Is Dependent upon Intact T Cell Signaling.

The requirement of T cell activation for vaccine efficacy against oxycodone was tested first in a genetic mouse model lacking functional TCR and then using a vaccine model lacking immunogenic T cell epitopes. Because TCRα knockout (TCR$\alpha^{-/-}$) mice are not available on the BALB/c background, we immunized control C57BL/6 WT and TCR$\alpha^{-/-}$, bred on C57BL/6 background, with OXY-KLH adsorbed on alum and boosted twice, 14 days apart. Serum antibodies were analyzed on day 35 post initial immunization. TCR$\alpha^{-/-}$ mice produced significantly lower levels of oxycodone-specific IgG antibodies $0.2 \pm 0 \times 10^3$ (mean ± SEM), compared to C57BL/6 WT controls, $84 \pm 25 \times 10^3$ (mean ± SEM, $p \leq 0.05$, Figure 2A). Previous studies have shown that carrier proteins can activate T cells, eliciting a more effective, T cell-dependent antibody production.[42] To further assess the contribution of the carrier protein in generating antibodies against opioids or other drugs of abuse, BALB/c mice were immunized with OXY-KLH or OXY conjugated to well-established T cell independent antigens [ficoll[43] and dextran[44]]. In this experiment, all mice were sc immunized with conjugates adsorbed on alum on days 0, 14 and 28 and serum collected on day 35 post initial immunization. OXY-ficoll and OXY-dextran produced negligible oxycodone-specific serum IgG titers, $0.234 \pm 0 \times 10^3$ (mean ± SEM, Figure 2B), compared to mice immunized with OXY-KLH, $34 \pm 4 \times 10^3$ (mean ± SEM, $p \leq 0.001$, Figure 2B). Collectively, these data demonstrate that intact T cell signaling as well as proteins or other immunogenic carriers containing T cell epitopes are required for vaccine efficacy.

Reduced Oxycodone Distribution to the Brain and Expansion of the Early Hapten-Specific B Cell Population in Mice Immunized with Oxycodone Conjugate Vaccines Containing Different Carrier Proteins.

Next, we tested whether vaccine efficacy could be improved through carrier protein selection. To this end, a series of conjugate vaccines consisting of the lead $OXY(Gly)_4$ hapten conjugated to KLH, EcoCRM, rTTHc,CRM_{197}, and TT was assessed for their efficacy against oxycodone in mice. BALB/c mice were sc immunized with immunogens

adsorbed on alum. The OXY-EcoCRM, OXY-rTTHc, OXY-CRM_{197}, and OXY-TT conjugate vaccines elicited titers of $187 \pm 31 \times 10^3$, $150 \pm 19 \times 10^3$, $251 \pm 44 \times 10^3$, and $331 \pm 88 \times 10^3$ (mean ± SEM, Figure 3A), respectively, which were significantly higher compared to the KLH control ($p \leq 0.001$) and OXY-KLH (OXY-CRM_{197} and OXY-TT only, $p \leq 0.05$). Analysis of the relative affinities of oxycodone-specific serum IgG antibodies by competitive ELISA indicated that, although there were no statistically significant differences across immunization groups, OXY- EcoCRM ($IC_{50} = 4.4 \pm 3.0 \times 10^{-7}$, mean ± SEM) and OXY-rTTHc ($IC_{50} = 0.95 \pm 4.9 \times 10^{-7}$) showed a trend toward increased affinity for oxycodone compared to the OXY-KLH group ($IC_{50} = 35.0 \pm 2.9 \times 10^{-7}$). Serum oxycodone concentrations were significantly increased in all groups 30 min after a 2.25 mg/kg oxycodone challenge, except for OXY-KLH, compared to KLH controls ($p \leq 0.05$, Figure 3B). Brain oxycodone concentrations were significantly reduced in all groups compared to KLH ($p < 0.0001$, Figure 3C). Consistent with previous reports,[21,35,39,41] there was a significant relationship between individual oxycodone-specific serum IgG titers and oxycodone concentrations in the brain of vaccinated mice ($r^2 = 0.30$, $p \leq 0.05$, Figure 3D).

Subsequently, we analyzed the B cell response specific for the oxycodone hapten in mice immunized with OXY-KLH, OXY-EcoCRM, OXY-rTTHc, and OXY-sKLH. Mice were IM immunized with 100 μg of conjugate immunogen and 250 μg alum. Spleen and lymph nodes were harvested 7 days post-immunization. Mice immunized with OXY-rTTHc displayed a significantly higher percentage of OXY-specific plasma B cells compared to KLH ($p \leq 0.05$, Figure 3E). Mice immunized with OXY-KLH and OXY-EcoCRM showed a significant increase in OXY-specific GC B cells compared to KLH control ($p \leq 0.01$, Figure 3F). Additionally, OXY-sKLH significantly increased the number of OXY-specific IgM^+ B cells compared to the control ($p \leq 0.001$, Figure S3A). Compared to control, all immunized groups consistently showed an elevated OXY-specific B cell response (Figure 3E,F, S3), suggesting that all carrier proteins supported B cell population expansion and differentiation necessary for generation of effective oxycodone-specific IgG antibodies.

Characterization of Conjugate Vaccines.

To test vaccines in human subjects, regulatory agencies (e.g., FDA) require the demonstration of batch-to-batch reproducibility and a physical and chemical qualification of the conjugates.[45] Of particular interest to development of conjugate vaccines, the molecular weight (MW) or size of the conjugates are used to determine the haptenation ratio of the conjugate. Unfortunately, determining the MW of large conjugates and characterizing the hapten-to-protein ratio, as well as the aggregation or degradation status, can be challenging. For well-established native and subunit KLH as well as TT.[21,39] instance, our group has developed opioid vaccines using the However, KLH conjugates are too large in MW for characterization by MALDI-TOF or other standard methods.[46] Instead, drug-conjugate vaccines containing smaller carrier proteins, such as BSA or OVA[39] and TT or $CRM_{197,}$[18] can be characterized by MALDI-TOF or other analytical assays.[47] In fact, conjugation conditions are often optimized using BSA and OVA in lieu of larger carrier proteins because it is easier to measure their haptenation ratio.[40,48–50]

Here, we performed a series of experiments to identify the most efficient assays to qualify each carrier protein and its respective conjugate vaccine. Unconjugated carrier proteins and conjugates were first analyzed using MALDI-TOF. This assay was effective at measuring the haptenation ratio of OXY-EcoCRM, OXY-rTTHc, and OXY-CRM_{197} (Figure 4), but did not resolve unconjugated TT or the conjugated OXY-TT (Figure 4D,H), which was likely due to the suboptimal quality or purity of this TT batch. Yet, OXY-TT was still effective in mice (Figure 3). Because of their larger MW, OXY-KLH and OXY-sKLH were not analyzed by MALDI-TOF.

Another challenge in development of hapten–protein conjugates is to qualify the presence or extent of aggregates, so that each conjugate batch can be validated to ensure reproducibility. MALDI-TOF does not discriminate potential aggregation, which may occur during or after conjugation. As an alternative method to MALDI-TOF, conjugates were analyzed by DLS, which showed the relative size of all conjugates compared to the carrier protein alone and the amount of aggregation (as a percent of total volume, Figure 5). Data showed increased particle size after conjugation, except for OXY-CRM_{197} (Figure 5A–E). Multiple peaks on the DLS graph (>100 nm) of EcoCRM, rTTHc, CRM_{197}, and KLH may be indicative of aggregates (Figure 5A–E). However, for EcoCRM and rTTHc, the suspected aggregates represented a small percentage of the total volume for both the unconjugated and conjugated carrier protein (Figure 5F,G). Furthermore, OXY-CRM_{197}, OXY-TT, and OXY-KLH displayed large diameter aggregates (Figure 5C,D,E), which accounted for ~10% of the volume of the conjugated protein solution (Figure 5H,I,J).

Subsequently, we used SEC-HPLC to characterize unconjugated EcoCRM, rTTHc, and their respective conjugates. SEC analysis indicated that the conjugates were not resolvable by this method, while the unconjugated EcoCRM and rTTHc eluted within the MW range of the column (Figure 6A–D). Using this method, the unconjugated EcoCRM and rTTHc yielded MW of 62.3 and 38.8 kDa, respectively, which were not consistent with the MW found by MALDI-TOF. The lower intensity peaks indicated the presence of small aggregates eluting through the column in both conjugated and unconjugated samples (Figure 6), which was consistent with the DLS data (Figure 5). Assessment of OXY-EcoCRM and OXY-rTTHc conjugates by SDS-PAGE did not demonstrate a defined band in the MW range of the gel (Figure 6E, lanes 3 and 5). However, the unconjugated EcoCRM and rTTHc were visible as indicated in Figure 6E, lanes 2 and 4. The gel confirms the presence of small aggregates in both the unconjugated and conjugated samples. Table 1 provides an overview of the analytical assays used to characterize oxycodone conjugate vaccines in this study.

Vaccines Containing either sKLH or EcoCRM Are Equally Effective against Heroin and Its Metabolites in Mice.

In this final experiment, heroin vaccines consisting of the M-sKLH and M-EcoCRM conjugates were tested for immunogenicity and efficacy in blocking opioid distribution to the brain in mice challenged sc with a heroin dose of 1 mg/kg. Both conjugates were characterized by DLS for size. The M-sKLH and M-EcoCRM vaccines included a lead morphine-based hapten (M) containing a tetraglycine linker for EDAC coupling chemistry.[20] Immunization with M-sKLH and M-EcoCRM elicited equivalent antibody titers (Figure

7A), which increased the retention of heroin, 6-AM, and morphine in the serum of vaccinated mice compared to the control ($p \leq 0.05$, Figure 7B). Both M-sKLH and M-EcoCRM reduced the cumulative concentration of heroin, 6-AM, and morphine in the brain respectively by 89 and 79% compared to the control ($p \leq 0.001$, Figure 7C). Both vaccine formulations were equally effective in reducing heroin-induced antinociception in the hot plate test (Figure 7D). For both vaccine conjugates, DLS analysis confirmed a peak shift in the size between the conjugate and their respective unconjugated carrier protein (Figure 7E,F). The DLS profile of the M-EcoCRM showed multiple peaks in the 10^2–10^4 nm range, which may indicate the presence of aggregates under current conjugation conditions (Figure 7F).

DISCUSSION

Vaccines may offer a promising strategy to treat OUD and possibly reduce the incidence of opioid-related fatal overdoses. Translation of candidate conjugate vaccines has often been challenging due to the limited availability of GMP-grade carrier proteins as well as the ability to characterize new conjugate vaccine products. The main findings of this study were that: (1) optimal vaccine efficacy against oxycodone was achieved by means of oxycodone-based haptens containing a tetraglycine linker at the C6 position and conjugated to carrier proteins using EDAC coupling chemistry; (2) the generation of oxycodone-specific serum IgG antibodies was contingent upon intact T cell signaling; (3) vaccines consisting of oxycodone haptens conjugated to EcoCRM, rTTHc, KLH or sKLH, TT, and CRM_{197} were equally effective in inducing hapten-specific B cell expansion and in reducing oxycodone distribution to the brain in mice; (4) vaccines containing EcoCRM, rTTHc, and CRM_{197} were characterized by MALDITOF and/or DLS, while vaccines containing either native KLH, sKLH, or TT were only qualified by DLS; and (5) these findings translated to heroin vaccines containing either EcoCRM or sKLH, which were effective against heroin and its metabolites in mice. Overall, this study identifies vaccine candidates and vaccine components suitable for further development and compares analytical assays for characterization of drug-carrier conjugate vaccines.

Hapten design and conjugation chemistry affect vaccine efficacy and selectivity against drugs of abuse.[18,50,51,34] In our experience, oxycodone-based haptens containing linkers at the C6 position provided more effective and selective immunogens than hydrocodone-based haptens modified either at the C6 or C8 position, regardless of using EDAC or maleimide coupling.[14] Additionally, vaccines containing a C6-derivatized oxycodone-based hapten containing tetraglycine linkers with a C-terminal carboxyl group (–COOH) for EDAC chemistry were more effective against oxycodone than vaccines containing a C6-derivatized oxycodone-based hapten with a shorter linker equipped with a thiol (–SH) group for maleimide chemistry.[14] Here, we further consolidated these previous observations by comparing C6-derivatized oxycodone-based haptens containing tetraglycine linkers of equal length equipped with either a terminal –COOH or a –SH group, which were conjugated to KLH by either EDAC or maleimide chemistry. The EDAC-conjugated $OXY(Gly)_4$-KLH vaccine outperformed its maleimide-conjugated equivalent (Figure 1), further supporting advancement of this lead oxycodone vaccine, which has previously been shown to be effective in reducing both oxycodone- and hydrocodone-induced antinociception and their

distribution to the brain in rats,[14] oxycodone intravenous self-administration in rats,[16] and oxycodone-induced respiratory depression and bradycardia in both mice and rats.[23,41] Another group reported the synthesis of oxycodone-and hydrocodone-based haptens modified at the *N*-methyl group with a succinic anhydride-derived linker conjugated to TT by EDAC chemistry, which were effective in reducing oxycodone- and hydrocodone-antinociception, their distribution to the brain, and their lethality in mice.[52] In a follow-up study, the OXY-TT vaccine containing the *N*-methyl group-derivatized linker conjugated with EDAC was effective in reducing oxycodone intravenous self-administration in rats.[48] These data highlight how linker composition and placement can affect vaccine efficacy against the target opioid. It has been shown that more B cells specific for C6-derivatized oxycodone-based haptens are present prior to immunization than B cells specific for C8-derivatized hydrocodone-based haptens, which correlates with vaccine efficacy against oxycodone in mice.[22] Indeed, the frequency of the precursor and early activated hapten-specific B cell subsets is predictive of individual vaccine efficacy against drugs of abuse.[22,35,36] Overall these data support further exploration of oxycodone-and hydrocodone-based haptens containing alternative linkers or placement positions to test whether vaccine design can achieve optimal B cell activation and enhance overall vaccine efficacy against these opioids.

To test alternative linker designs, this study also compared C6-modified oxycodone haptens containing a polyethylene glycol linker of length equivalent to the tetraglycine linker. Despite previous reports supporting the use of PEGylated linkers [$(PEG)_2$-maleimide cross-linker],[18] we found that PEGylated linkers were not a viable option for development of effective oxycodone vaccines (Figure 1). The lack of efficacy of the vaccine containing the $OXY(PEG)_3$ hapten may be attributed to PEGylated products propensity to degrade overtime in biological samples[53] or because the tetraglycine linker provides more context to B cell recognition. It has been hypothesized that peptide linkers may provide additional recognition sites for cognate B and T cells.[51] The addition of glycine linkers has been shown to increase antibody affinity and concentration compared to the same hapten with no linker.[51] In fact, tetraglycine linkers have been successfully used in generation of vaccines targeting heroin and its metabolites.[15,20]

As stated above, the choice of conjugation chemistry is a critical milestone in conjugate vaccine development. The two main conjugation chemistry approaches consist of carbodiimide and maleimide coupling.[54] Conjugation chemistry can yield different haptenation ratios, depending upon the individual hapten and protein being conjugated, which affects the quantity and quality of the drug-specific response and vaccine efficacy against the target drug of abuse.[55] Although both carbodiimide and maleimide chemistry have been used to generate effective vaccines against heroin, hydrocodone, oxycodone, and fentanyl, overall evidence suggests marginal superiority of EDAC-based conjugations.[56,10,24,14,24] However, choice of EDAC versus maleimide may depend upon individual hapten:carrier conjugates, or whether the hapten synthesis may be restricted to include a terminal –SH group.[18,57] Hence, it is appropriate to evaluate alternative coupling chemistries to identify lead hapten designs.

As generation of effective drug-specific antibodies depends upon hapten-specific B cells, activation of B cells is dependent upon appropriate cognate $CD4^+$ T cell stimulation.[28] It has been previously shown that depletion of $CD4^+$ T cells blunts hapten-specific B cell activation and vaccine efficacy against oxycodone,[35] and that the frequency of carrier-specific MHCII-restricted $CD4^+$ T cells relates to vaccine efficacy.[35] This study extends this notion by showing that oxycodone-specific serum IgG antibodies are not generated in a genetic mouse model lacking a functional TCR, or in WT mice immunized with OXY haptens conjugated to dextran and ficoll, which are well-established models to test for evidence of T cell-independent B cell activation (Figure 2). These data reinforce the concept that immunogenic carriers are needed, and that carriers need to incorporate T cell epitopes.

Carriers are usually bacterial or viral proteins, or other foreign macromolecules that stimulate host innate and adaptive immunity.[28] Approved vaccines against pathogens contain well-characterized carrier proteins, including diphtheria toxoid (DT), CRM_{197}, TT, meningococcal outer membrane protein complex (OMPC), and *Haemophilus influenzae* protein D (HiD).[42] Other carrier proteins, such as sKLH, have been tested in clinical trials, but not yet approved.[58] The field of addiction vaccines has tested a variety of well-established carrier proteins, such as CRM_{197}, TT, cholera toxin B, and recombinant Exotoxin A from *Pseudomonas aeruginosa* (rEPA), as well as novel carriers, including the TLR5 agonist flagellin,[59] liposomes,[60] peptide nanofibers,[61] virus-like particles,[62] disrupted adeno-associated viruses,[63,64] nanoparticles,[65] and other platforms.[28,29] Despite promising preclinical efficacy for these approaches, carrier proteins are still most likely to offer an easier path to regulatory approval. However, it is challenging or costly to secure GMP-grade proteins, as well as other vaccine components, such as adjuvants, from the private sector. Our experience in early stage development of heroin and oxycodone vaccines has focused on native KLH, which is often difficult to characterize because of its high MW,[66] and it is not available under GMP. To address these limitations, our late-stage development efforts have focused on candidate oxycodone and heroin vaccines containing GMP-grade subunit KLH or alternatively TT.[21,67] Hence, it is of interest to test alternative vaccine components as they become available, which may inform or speed translation and future product development.

This study showed that the lead OXY hapten conjugated to KLH, EcoCRM, rTTHc, TT, and CRM_{197} was equally effective in reducing distribution to the brain of a clinically relevant dose of oxycodone (Figure 3). These conjugates were also effective in inducing early OXY-specific B cell expansion, which is an established marker predictive of individual vaccine efficacy (Figure 3).[35] Consistent with previous data, higher oxycodone-specific IgG antibody titers were correlated with individual vaccine efficacy against oxycodone. In addition, mice vaccinated with OXY-rTTHc displayed marginal protection against opioid-induced respiratory depression compared to control (Supplemental Figure 4).

Here, these conjugates were characterized by different analytical assays to assess their MW and haptenation ratio as well as to qualify potential aggregation or degradation. MALDI-TOF is the standard technique for characterization of small molecule haptens conjugated to carrier proteins.[68] In this study, MALDI-TOF allowed qualification of the OXY-EcoCRM (HR = 24), OXY-rTTHc (HR = 15), and OXY-CRM_{197} (HR = 28) conjugates but not of OXY-TT or OXY-KLH conjugates (Figure 4). These results are consistent with the previous

assessment of OXY haptens conjugated to BSA (HR = 16–21),[14,39] and other opioid conjugates.[50] Although ideal for characterization of the haptenation ratio of smaller conjugates, MALDI-TOF is not well-suited to analyze larger conjugates (e.g., OXY-KLH) or to qualify the extent of conjugate aggregation.

As an alternative to MALDI-TOF, DLS is used to measure particle size and size distribution, thereby qualitatively assessing potential aggregation/degradation of conjugate products. Here, DLS was used to validate conjugation of OXY haptens to carrier proteins as well as assess conjugate homogeneity. When peaks observed in the intensity plots (Figure 5A–E), indicating the product size, were compared to the percent of the volume (Figure 5F–J), indicating the relative amount of each peak, we found that OXY-EcoCRM, OXY-rTTHc, and OXY-KLH conjugates had the largest percentage of homogeneous product. It is generally accepted, but not often systematically investigated, that immunogens of higher aggregation status and larger size are more effective in inducing antibody responses. Previous studies tested this hypothesis by immunizing subjects with several batches of nicotine vaccines displaying various degrees of aggregation, and found that the extent of aggregation (and other physical chemical properties of the conjugates) correlated with individual vaccine efficacy against nicotine in both mice and nonhuman primates.[69–71]

Finally, because SEC-HPLC and SDS PAGE are routinely used to qualify commercial proteins, these assays were included in our assessment. Both SEC-HPLC and SDS PAGE provided an approximate MW for EcoCRM and rTTHc (Figure 6) within previously published ranges[37,72] Unfortunately, these MW did not match the data obtained from MALDI-TOF. Since the conjugated products were not resolvable by SEC-HPLC and SDS PAGE under current conditions, we calculated the haptenation ratios of the conjugates based upon the MALDI-TOF analysis, as described in Table 1. We hypothesize that the size or the charge of the conjugates may have affected their ability to pass through columns and electrophoresis gels. For instance, size complicates the characterization of the OXY-KLH conjugates. However, this may not be the case for OXY-EcoCRM and OXY-rTTHc, since these conjugates were characterized by MALDI-TOF. Furthermore, we have previously characterized nicotine–KLH conjugates by agarose gel electrophoresis,[73] while we were not successful in using gel electrophoresis for analysis of other opioid–KLH conjugates (Pravetoni, *personal communication*). Another group was able to qualify morphine–TT conjugates by nonreducing SDS PAGE and native PAGE,[50] suggesting that the hapten structure and the PAGE conditions affect the analysis of drug–protein conjugates by gel electrophoresis. Since haptens derived from opioids, nicotine, or other drugs of abuse may have different chemical structures, we hypothesize that charge or other physical chemical properties of the conjugates (e.g., globularity) may be the limiting factor for characterization by SEC and PAGE. These data indicate that individual conjugates shall be assessed by various analytical assays, and results may vary according to the MW, choice of the carrier protein, and the physical chemical properties of the hapten.

Finally, findings were generalized to the development of heroin vaccines by conjugating the lead $M(Gly)_4$ hapten to the sKLH and EcoCRM carrier proteins. We have previously shown that the $M(Gly)_4$ hapten conjugated to KLH and sKLH using EDAC chemistry effectively reduced the behavioral effects of heroin in rodents, including heroin self-administration and

heroin-induced locomotor activity.[15,67] Here, heroin vaccines containing either EcoCRM or sKLH were equally effective in reducing heroin-induced antinociception and distribution to the brain of heroin and its metabolites 6AM and morphine in mice. Both M-EcoCRM and M-sKLH were characterized by DLS, proving that this analytical assay is useful to qualify a variety of conjugate products for their size, and that both EcoCRM and sKLH are equally effective vaccine components suitable for development of conjugate vaccines against opioids and possibly other drugs of abuse.

In conclusion, this study demonstrates that the lead OXY$(Gly)_4$OH and M$(Gly)_4$OH haptens equipped with a terminal carboxyl group for EDAC coupling chemistry show conserved efficacy against either oxycodone or heroin when conjugated to various carrier proteins. Finally, EcoCRM and rTTHc offer valid alternatives to previously established KLH, sKLH, TT, and CRM_{197} carrier proteins. Future studies will focus on comparing opioid vaccine formulations containing these carrier proteins in other animal models to further support translation of vaccines to treat OUD and reduce opioid fatal overdoses.

Supplementary Material

Refer to Web version on PubMed Central for supplementary material.

ACKNOWLEDGMENTS

We thank Drs. Maria Luisa Gelmi and Francesca Clerici for establishing an institutional and educational agreement between the Facoltà di Scienze del Farmaco, Università degli Studi di Milano, and the University of Minnesota Medical School.

ABBREVIATIONS USED

CRM_{197}	cross-reactive material
Eco	*E. coli*-expressed
ELISA	enzyme-linked immunosorbent assay
FDA	Food and Drug Administration
GMP	good manufacturing practices
KLH	keyhole limpet hemocyanin
M	morphine-based hapten
OUD	opioid use disorders
OXY	oxycodone-based hapten
sKLH	subunit keyhole limpet hemocyanin
rTTHc	tetanus toxin heavy chain fragment C
TT	tetanus toxoid

REFERENCES

(1). World Drug Report 2018 https://www.unodc.org/wdr2018/index.html.

(2). Butler DC; Shanks K; Behonick GS; Smith D; Presnell SE; Tormos LM Three Cases of Fatal Acrylfentanyl Toxicity in the United States and a Review of Literature. J. Anal. Toxicol 2018, 42 (1), e6–e11. [PubMed: 29036502]

(3). Helander A; Backberg M; Signell P; Beck O Intoxications involving acrylfentanyl and other novel designer fentanyls - results from the Swedish STRIDA project. Clin. Toxicol 2017, 55 (6), 589–599.

(4). Tam T Commentary - Building the evidence base for sustained public health response to the opioid epidemic in Canada. Health Promot Chronic Dis Prev Can. 2018, 38 (6), 221–222. [PubMed: 29911817]

(5). Key substance use and mental health indicators in the United States: Results from the 2016 National Survey on Drug Use and Health (HHS Publication No. SMA 17–5044, NSDUH Series H-52); Center for Behavioral Health Statistics and Quality, Substance Abuse and Mental Health Services Administration: Rockville, 2017.

(6). Drugs Involved in U.S. Overdose Deaths, 2000–2016. https://www.drugabuse.gov/related-topics/trends-statistics/overdose-deathrates (accessed February 01, 2018).

(7). Rhyan C The Potential Societal Benefit Of Eliminating The Opioid Crisis Exceeds $95 Billion Per Year; Research Brief for Altarum, 11 16, 2017.

(8). CDC. Wide-ranging OnLine Data for Epidemiologic Research (WONDER);Center for Disease Control and Prevention Department of Health & Human Services, 2012.

(9). Volkow ND; Collins FS The Role of Science in Addressing the Opioid Crisis. N. Engl. J. Med 2017, 377 (4), 391–394. [PubMed: 28564549]

(10). Stowe GN; Schlosburg JE; Vendruscolo LF; Edwards S; Misra KK; Schulteis G; Zakhari JS; Koob GF; Janda KD DEVELOPING A VACCINE AGAINST MULTIPLE PSYCHOACTIVE TARGETS: A CASE STUDY OF HEROIN. CNS Neurol. Disord.: Drug Targets 2011, 10 (8), 865–875. [PubMed: 22229311]

(11). Bremer PT; Kimishima A; Schlosburg JE; Zhou B; Collins KC; Janda KD Combatting synthetic designer opioids: active vaccination ablates lethal doses of fentanyl class drugs. Angew. Chem., Int. Ed 2016, 55 (11), 3772–3775.

(12). Schlosburg JE; Vendruscolo LF; Bremer PT; Lockner JW; Wade CL; Nunes AAK; Stowe GN; Edwards S; Janda KD; Koob GF Dynamic vaccine blocks relapse to compulsive intake of heroin. Proc. Natl. Acad. Sci. U. S. A 2013, 110 (22), 9036–9041. [PubMed: 23650354]

(13). Li Q-Q; Sun C-Y; Luo Y-X; Xue Y-X; Meng S-Q; Xu L-Z; Chen N; Deng J-H; Zhai H-F; Kosten TR; Shi J; Lu L; Sun H-Q A Conjugate Vaccine Attenuates Morphine- and Heroin-Induced Behavior in Rats. Int. J. Neuropsychopharmacol 2015, 18 (5), pyu093.

(14). Pravetoni M; Le Naour M; Tucker AM; Harmon TM; Hawley TM; Portoghese PS; Pentel PR Reduced Antinociception of Opioids in Rats and Mice by Vaccination with Immunogens Containing Oxycodone and Hydrocodone Haptens. J. Med. Chem 2013, 56 (3), 915–923. [PubMed: 23249238]

(15). Raleigh MD; Pravetoni M; Harris AC; Birnbaum AK; Pentel PR Selective Effects of a Morphine Conjugate Vaccine on Heroin and Metabolite Distribution and Heroin-Induced Behaviors in Rats. J. Pharmacol. Exp. Ther 2013, 344 (2), 397–406. [PubMed: 23220743]

(16). Pravetoni M; Pentel PR; Potter DN; Chartoff EH; Tally L; LeSage MG Effects of an Oxycodone Conjugate Vaccine on Oxycodone Self-Administration and Oxycodone-Induced Brain Gene Expression in Rats. PLoS One 2014, 9 (7), e101807. [PubMed: 25025380]

(17). Raleigh MD; Pentel PR; LeSage MG Pharmacokinetic Correlates of the Effects of a Heroin Vaccine on Heroin SelfAdministration in Rats. PLoS One 2014, 9 (12), e115696. [PubMed: 25536404]

(18). Jalah R; Torres OB; Mayorov AV; Li F; Antoline JFG; Jacobson AE; Rice KC; Deschamps JR; Beck Z; Alving CR; Matyas GR Efficacy, but not antibody titer or affinity, of a heroin hapten conjugate vaccine correlates with increasing hapten densities on tetanus toxoid, but not on CRM(197) carriers. Bioconjugate Chem. 2015, 26 (6), 1041–1053.

(19). Bremer PT; Schlosburg JE; Lively JM; Janda KD Injection Route and TLR9 Agonist Addition Significantly Impact Heroin Vaccine Efficacy. Mol. Pharmaceutics 2014, 11 (3), 1075–1080.

(20). Pravetoni M; Raleigh MD; Le Naour M; Tucker AM; Harmon TM; Jones JM; Birnbaum AK; Portoghese PS; Pentel PR Co-administration of morphine and oxycodone vaccines reduces the distribution of 6-monoacetylmorphine and oxycodone to brain in rats. Vaccine 2012, 30 (31), 4617–4624. [PubMed: 22583811]

(21). Pravetoni M; Vervacke JS; Distefano MD; Tucker AM; Laudenbach M; Pentel PR Effect of Currently Approved Carriers and Adjuvants on the Pre-Clinical Efficacy of a Conjugate Vaccine against Oxycodone in Mice and Rats. PLoS One 2014, 9 (5), e96547. [PubMed: 24797666]

(22). Taylor JJ; Laudenbach M; Tucker AM; Jenkins MK; Pravetoni M Hapten-specific naive B-cells are biomarkers of vaccinë efficacy against drugs of abuse. J. Immunol. Methods 2014, 405, 74–86. [PubMed: 24462800]

(23). Raleigh MD; Peterson SJ; Laudenbach M; Baruffaldi F; Carroll FI; Comer SD; Navarro HA; Langston TL; Runyon SP; Winston S; Pravetoni M; Pentel PR Safety and efficacy of an oxycodone vaccine: Addressing some of the unique considerations posed by opioid abuse. PLoS One 2017, 12 (12), e0184876. [PubMed: 29194445]

(24). Bremer PT; Schlosburg JE; Banks ML; Steele FF; Zhou B; Poklis JL; Janda KD Development of a Clinically Viable Heroin Vaccine. J. Am. Chem. Soc 2017, 139 (25), 8601–8611. [PubMed: 28574716]

(25). Sulima A; Jalah R; Antoline JFG; Torres OB; Imler GH; Deschamps JR; Beck Z; Alving CR; Jacobson AE; Rice KC; Matyas GR A Stable Heroin Analogue That Can Serve as a Vaccine Hapten to Induce Antibodies That Block the Effects of Heroin and Its Metabolites in Rodents and That Cross-React Immunologically with Related Drugs of Abuse. J. Med. Chem 2018, 61 (1), 329–343. [PubMed: 29236495]

(26). Hatsukami DK; Jorenby DE; Gonzales D; Rigotti NA; Glover ED; Oncken CA; Tashkin DP; Reus VI; Akhavain RC; Fahim RE; Kessler PD; Niknian M; Kalnik MW; Rennard SI Immunogenicity and smoking-cessation outcomes for a novel nicotine immunotherapeutic. Clin. Pharmacol. Ther 2011, 89 (3), 392–9. [PubMed: 21270788]

(27). Martell BA; Orson FM; Poling J; Mitchell E; Rossen RD; Gardner T; Kosten TR Cocaine Vaccine for the Treatment of Cocaine Dependence in Methadone Maintained Patients: A Randomized Double-Blind Placebo-Controlled Efficacy Trial. Arch. Gen. Psychiatry 2009, 66 (10), 1116–23. [PubMed: 19805702]

(28). Pravetoni M Biologics to treat substance use disorders: Current status and new directions. In Human Vaccines & Immunotherapeutics; Taylor & Francis, 2016; Vol. 12, pp 3005–3019.

(29). Pentel PR; LeSage MG New directions in nicotine vaccine design and use. Adv. Pharmacol 2014, 69, 553–80. [PubMed: 24484987]

(30). Skolnick P Biologic Approaches to Treat Substance Use Disorders. Trends Pharmacol. Sci 2015, 36 (10), 628–35. [PubMed: 26435208]

(31). Akbarzadeh A; Norouzian D; Farhangi A; Mehrabi MR; Chiani M; et al.etal Immunotherapy of 347 volunteer outpatients morphine addicts by human therapeutic morphine vaccine in Kermanshah Province of Iran. J. Pharmacol. Toxicol 2009, 4, 30–35.

(32). Montoya ID Advances in the development of biologics to treat drug addictions and overdose. Adicciones 2012, 24 (2), 95–103. [PubMed: 22648312]

(33). Bremer PT; Janda KD Conjugate Vaccine Immunotherapy for Substance Use Disorder. Pharmacol. Rev 2017, 69 (3), 298–315. [PubMed: 28634286]

(34). Pryde DC; Jones LH; Gervais DP; Stead DR; Blakemore DC; Selby MD; Brown AD; Coe JW; Badland M; Beal DM; Glen R; Wharton Y; Miller GJ; White P; Zhang N; Benoit M; Robertson K; Merson JR; Davis HL; McCluskie MJ Selection of a novel anti-nicotine vaccine: influence of antigen design on antibody function in mice. PLoS One 2013, 8 (10), e76557. [PubMed: 24098532]

(35). Laudenbach M; Baruffaldi F; Vervacke JS; Distefano MD; Titcombe PJ; Mueller DL; Tubo NJ; Griffith TS; Pravetoni M The frequency of naïve and early-activated hapten- specific B-cell subsets dictates the efficacy of a therapeutic vaccine against prescription opioid abuse. J. Immunol 2015, 194 (12), 5926–5936. [PubMed: 25972483]

(36). Laudenbach M; Tucker AM; Runyon SP; Carroll FI; Pravetoni M The frequency of early-activated hapten-specific B-cell subsets predicts the efficacy of vaccines for nicotine dependence. Vaccine 2015, 33 (46), 6332–6339. [PubMed: 26409811]

(37). Hickey JM; Toprani VM; Kaur K; Mishra RPN; Goel A; Oganesyan N; Lees A; Sitrin R; Joshi SB; Volkin DB Analytical Comparability Assessments of Five Recombinant CRM_{197} Proteins from Different Manufacturers and Expression Systems. J. Pharm. Sci 2018, 107, 1806. [PubMed: 29526446]

(38). Halpern JL; Habig WH; Neale EA; Stibitz S Cloning and expression of functional fragment C of tetanus toxin. Infect. Immun 1990, 58 (4), 1004–1009. [PubMed: 2318526]

(39). Pravetoni M; Le Naour M; Harmon TM; Tucker AM; Portoghese PS; Pentel PR An Oxycodone Conjugate Vaccine Elicits Drug-Specific Antibodies that Reduce Oxycodone Distribution to Brain and Hot-Plate Analgesia. J. Pharmacol. Exp. Ther 2012, 341 (1), 225–232. [PubMed: 22262924]

(40). Pravetoni M; Keyler DE; Pidaparthi RR; Carroll FI; Runyon SP; Murtaugh MP; Earley CA; Pentel PR Structurally distinct nicotine immunogens elicit antibodies with nonoverlapping specificities. Biochem. Pharmacol 2012, 83 (4), 543–550. [PubMed: 22100986]

(41). Laudenbach M; Baruffaldi F; Robinson C; Carter P; Seelig D; Baehr C; Pravetoni M Blocking interleukin-4 enhances efficacy of vaccines for treatment of opioid abuse and prevention of opioid overdose. Sci. Rep 2018, 8, 5508. [PubMed: 29615715]

(42). Pichichero ME Protein carriers of conjugate vaccines: Characteristics, development, and clinical trials. Hum. Vaccines Immunother 2013, 9 (12), 2505–2523.

(43). Vinuesa CG; Sze DM; Cook MC; Toellner KM; Klaus GG; Ball J; MacLennan IC Recirculating and germinal center B-cells differentiate into cells responsive to polysaccharide antigens. Eur. J. Immunol 2003, 33 (2), 297–305. [PubMed: 12548560]

(44). Wang D; Wells SM; Stall AM; Kabat EA Reaction of germinal centers in the T-cell-independent response to the bacterial polysaccharide alpha(1–>6)dextran. Proc. Natl. Acad. Sci. U. S. A 1994, 91 (7), 2502–6. [PubMed: 7511812]

(45). Guidance for Industry. Guidance for industry: Q6B specifications: test procedures and acceptance criteria for biotechnological /biological products; U.S. Department of Health and Human Services, Food and Drug Administration, Center for Drug Evaluation and Research: 1999.

(46). Gatsogiannis C; Markl J Keyhole Limpet Hemocyanin: 9-Å CryoEM Structure and Molecular Model of the KLH1 Didecamer Reveal the Interfaces and Intricate Topology of the 160 Functional Units. J. Mol. Biol 2009, 385 (3), 963–983. [PubMed: 19013468]

(47). Thorn JM; Bhattacharya K; Crutcher R; Sperry J; Isele C; Kelly B; Yates L; Zobel J; Zhang N; Davis HL; McCluskie MJ The Effect of Physicochemical Modification on the Function of Antibodies Induced by Anti-Nicotine Vaccine in Mice. Vaccines 2017, 5 (2), 11.

(48). Nguyen JD; Hwang CS; Grant Y; Janda KD; Taffe MA Prophylactic vaccination protects against the development of oxycodone self-administration. Neuropharmacology 2018, 138, 292–303. [PubMed: 29936242]

(49). Hwang CS; Bremer PT; Wenthur CJ; Ho SO; Chiang S; Ellis B; Zhou B; Fujii G; Janda KD Enhancing Efficacy and Stability of an Antiheroin Vaccine: Examination of Antinociception, Opioid Binding Profile, and Lethality. Mol. Pharmaceutics 2018, 15 (3), 1062–1072.

(50). Torres OB; Jalah R; Rice KC; Li F; Antoline JFG; Iyer MR; Jacobson AE; Boutaghou MN; Alving CR; Matyas GR Characterization and optimization of heroin hapten-BSA conjugates: method development for the synthesis of reproducible hapten-based vaccines. Anal. Bioanal. Chem 2014, 406 (24), 5927–5937. [PubMed: 25084736]

(51). Collins KC; Janda KD Investigating Hapten Clustering as a Strategy to Enhance Vaccines against Drugs of Abuse. Bioconjugate Chem. 2014, 25 (3), 593–600.

(52). Kimishima A; Wenthur CJ; Zhou B; Janda KD An Advance in Prescription Opioid Vaccines: Overdose Mortality Reduction and Extraordinary Alteration of Drug Half-Life. ACS Chem. Biol 2017, 12 (1), 36–40. [PubMed: 28103678]

(53). Mishra S; Webster P; Davis ME PEGylation significantly affects cellular uptake and intracellular trafficking of non-viral gene delivery particles. Eur. J. Cell Biol 2004, 83 (3), 97–111. [PubMed: 15202568]

(54). Stephanopoulos N; Francis MB Choosing an effective protein bioconjugation strategy. Nat. Chem. Biol 2011, 7 (12), 876–84. [PubMed: 22086289]

(55). Carroll FI; Blough BE; Pidaparthi RR; Abraham P; Gong PK; Deng L; Huang X; Gunnell M; Lay JO; Peterson EC; Owens SM Synthesis of Mercapto (+) methamphetamine Haptens and Their Use for Obtaining Improved Epitope Density on (+) Methamphetamine Conjugate Vaccines. J. Med. Chem 2011, 54 (14), 5221–5228. [PubMed: 21682289]

(56). Sulima A; Jalah R; Antoline JFG; Torres OB; Imler GH; Deschamps JR; Beck Z; Alving CR; Jacobson AE; Rice KC; Matyas GR A Stable Heroin Analogue That Can Serve as a Vaccine Hapten to Induce Antibodies That Block the Effects of Heroin and Its Metabolites in Rodents and That Cross-React Immunologically with Related Drugs of Abuse. J. Med. Chem 2018, 61 (1), 329–343. [PubMed: 29236495]

(57). Chen F; Nielsen S; Zenobi R Understanding chemical reactivity for homo- and heterobifunctional protein cross-linking agents. J. Mass Spectrom 2013, 48 (7), 807–12. [PubMed: 23832936]

(58). Stellar Biotechnologies, I. KLH Site, Keyhole Limpet Hemocyanin Knowledge Base. http://www.klhsite.org/klh-clinicaltrials/(accessed February, 27, 2018).

(59). Kimishima A; Wenthur CJ; Eubanks LM; Sato S; Janda KD Cocaine Vaccine Development: Evaluation of Carrier and Adjuvant Combinations That Activate Multiple Toll-Like Receptors. Mol. Pharmaceutics 2016, 13 (11), 3884–3890.

(60). Matyas GR; Mayorov AV; Rice KC; Jacobson AE; Cheng K; Iyer MR; Li F; Beck Z; Janda KD; Alving CR Liposomes Containing Monophosphoryl Lipid A: A Potent Adjuvant System For Inducing Antibodies To Heroin Hapten Analogs. Vaccine 2013, 31 (26), 2804–2810. [PubMed: 23624097]

(61). Rudra JS; Ding Y; Neelakantan H; Ding C; Appavu R; Stutz S; Snook JD; Chen H; Cunningham KA; Zhou J Suppression of Cocaine-Evoked Hyperactivity by Self-Adjuvanting and Multivalent Peptide Nanofiber Vaccines. ACS Chem. Neurosci 2016, 7 (5), 546–552. [PubMed: 26926328]

(62). Cornuz J; Zwahlen S; Jungi WF; Osterwalder J; Klingler K; van Melle G; Bangala Y; Guessous I; Müller P; Willers J; Maurer P; Bachmann MF; Cerny T A Vaccine against Nicotine for Smoking Cessation: A Randomized Controlled Trial. PLoS One 2008, 3 (6), e2547. [PubMed: 18575629]

(63). Hicks MJ; De BP; Rosenberg JB; Davidson JT; Moreno AY; Janda KD; Wee S; Koob GF; Hackett NR; Kaminsky SM; Worgall S; Toth M; Mezey JG; Crystal RG Cocaine analog coupled to disrupted adenovirus: a vaccine strategy to evoke high-titer immunity against addictive drugs. Mol. Ther 2011, 19 (3), 612–9. [PubMed: 21206484]

(64). Evans SM; Foltin RW; Hicks MJ; Rosenberg JB; De BP; Janda KD; Kaminsky SM; Crystal RG Efficacy of an adenovirus-based anti-cocaine vaccine to reduce cocaine self-administration and reacqusition using a choice procedure in rhesus macaques. Pharmacol., Biochem. Behav 2016, 150–151, 76–86.

(65). Hu Y; Zheng H; Huang W; Zhang C A novel and efficient nicotine vaccine using nano-lipoplex as a delivery vehicle. Hum. Vaccines Immunother. 2014, 10 (1), 64–72.

(66). Harris JR; Markl J Keyhole limpet hemocyanin (KLH): a biomedical review. Micron 1999, 30 (6), 597–623. [PubMed: 10544506]

(67). Raleigh MD; Laudenbach M; Baruffaldi F; Peterson SJ; Roslawski MJ; Birnbaum AK; Carroll FI; Runyon SP; Winston S; Pentel PR; Pravetoni M Opioid Dose- and RouteDependent Efficacy of Oxycodone and Heroin Vaccines in Rats. J. Pharmacol. Exp. Ther 2018, 365 (2), 346–353. [PubMed: 29535156]

(68). Singh KV; Kaur J; Varshney GC; Raje M; Suri CR Synthesis and characterization of hapten-protein conjugates for antibody production against small molecules. Bioconjugate Chem. 2004, 15 (1), 168–73.

(69). Thorn JM; Bhattacharya K; Crutcher R; Sperry J; Isele C; Kelly B; Yates L; Zobel J; Zhang N; Davis HL; McCluskie MJ The Effect of Physicochemical Modification on the Function of Antibodies Induced by Anti-Nicotine Vaccine in Mice. Vaccines (Basel, Switz.) 2017, 5 (2), E11.

(70). McCluskie MJ; Thorn J; Gervais DP; Stead DR; Zhang N; Benoit M; Cartier J; Kim IJ; Bhattacharya K; Finneman JI; Merson JR; Davis HL Anti-nicotine vaccines: Comparison of adjuvanted CRM197 and Qb-VLP conjugate formulations for immunogenicity and function in non-human primates. Int. Immunopharmacol 2015, 29 (2), 663–671. [PubMed: 26404190]

(71). McCluskie MJ; Thorn J; Mehelic PR; Kolhe P; Bhattacharya K; Finneman JI; Stead DR; Piatchek MB; Zhang N; Chikh G; Cartier J; Evans DM; Merson JR; Davis HL Molecular attributes of conjugate antigen influence function of antibodies induced by anti-nicotine vaccine in mice and non-human primates. Int. Immunopharmacol 2015, 25 (2), 518–527. [PubMed: 25737198]

(72). Helting TB; Zwisler O Structure of tetanus toxin. I. Breakdown of the toxin molecule and discrimination between polypeptide fragments. J. Biol. Chem 1977, 252 (1), 187–193. [PubMed: 401808]

(73). Pravetoni M; Keyler DE; Pidaparthi RR; Carroll FI; Runyon SP; Murtaugh MP; Earley CA; Pentel PR Structurally distinct nicotine immunogens elicit antibodies with nonoverlapping specificities. Biochem. Pharmacol 2012, 83 (4), 543–50. [PubMed: 22100986]

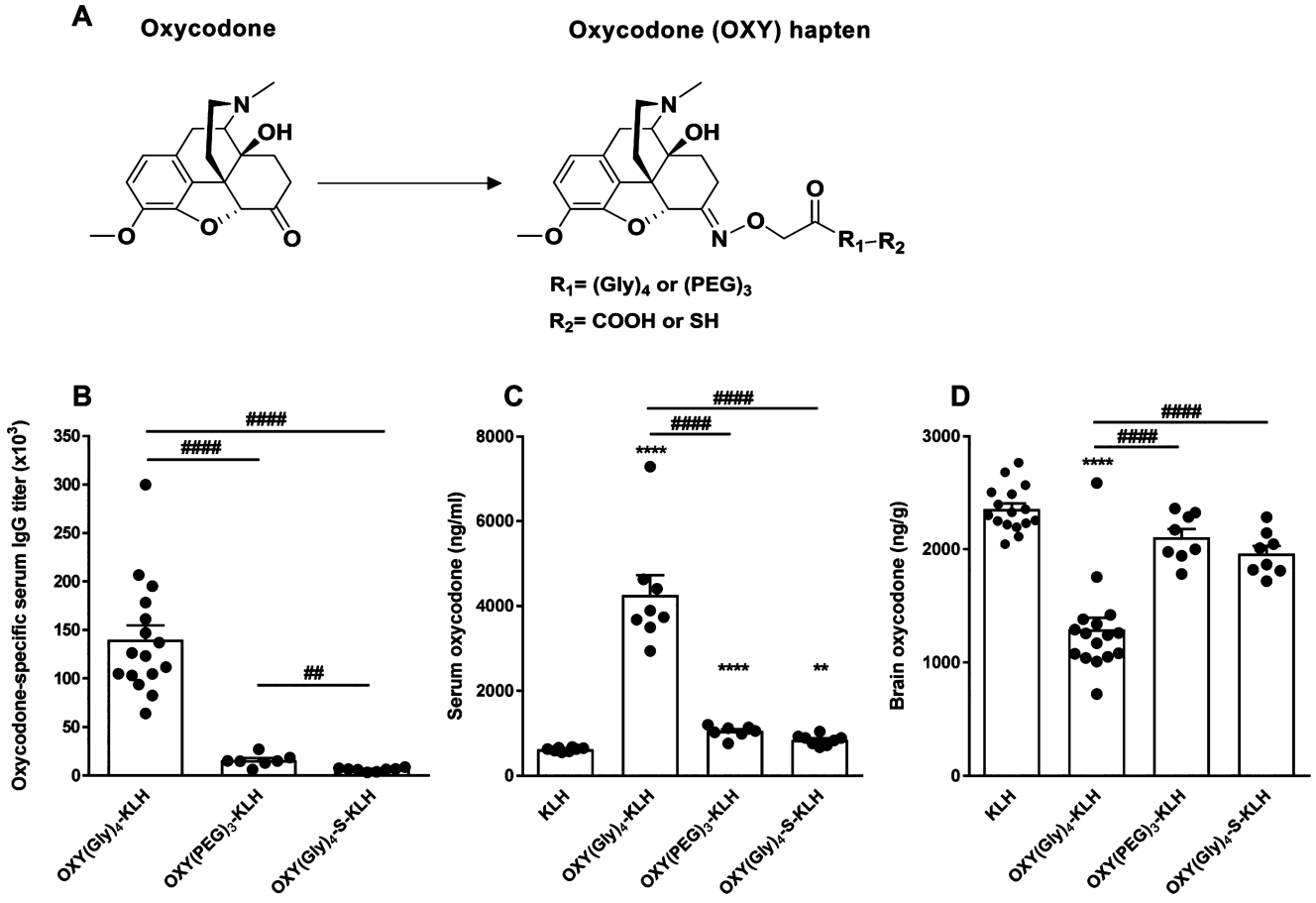

Figure 1.

Effect of hapten design and linker chemistry on vaccine efficacy against oxycodone in mice. (A) Structure of oxycodone and oxycodone-based haptens. BALB/c mice ($n \geq 7$/group) were immunized with unconjugated KLH control, OXY$(Gly)_4$-KLH, OXY$(PEG)_3$-KLH, or OXY$(Gly)_4$-S-KLH adsorbed on alum on days 0, 14, and 28. Vaccine efficacy was evaluated on day 35. (B) Oxycodone-specific serum IgG antibody titers. Oxycodone concentrations in (C) serum and (D) brain at 30 min after a 2.25 mg/kg sc oxycodone challenge. Data are mean ± SEM. Statistical symbols: * represents experimental groups compared to the KLH-only negative control, and # represents between group comparisons. ** or *##*, $p \leq 0.01$, and **** or *####*, $p \leq 0.0001$, using two-tailed unpaired t tests with Welch's correction (B, C, D) and a log-transformed, one-way ANOVA paired with Tukey's multiple comparison test (C, D).

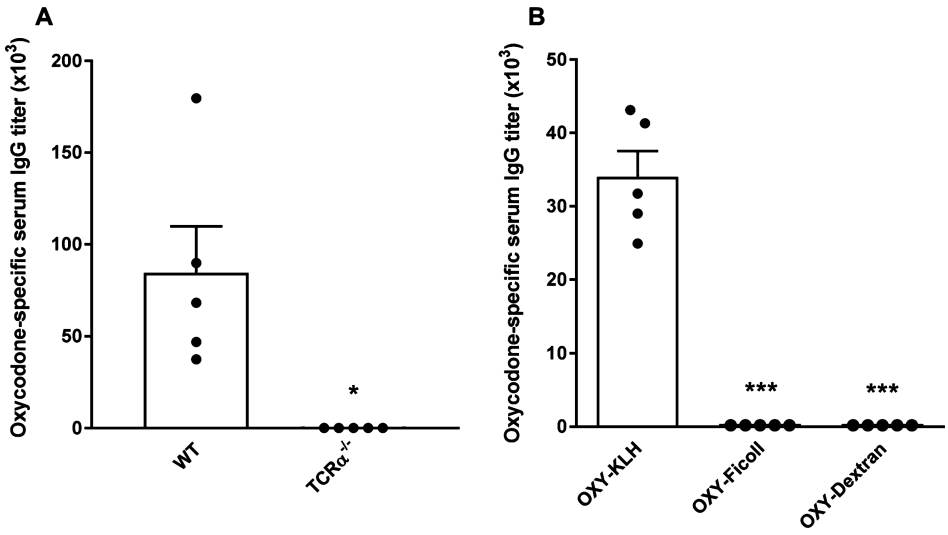

Figure 2.

Vaccine efficacy requires intact T cell signaling. Serum was collected on day 35, and oxycodone-specific IgG titers were analyzed via ELISA after the following immunizations. (A) C57BL/6 WT and TCR$\alpha^{-/-}$ mice (n = 5/group) were sc immunized with OXY(Gly)$_4$-KLH adsorbed on alum on days 0, 14, and 28. (B) BALB/c mice (n = 5/group) were sc immunized with OXY(Gly)$_4$-KLH, OXY-Ficoll, or OXY-Dextran adsorbed on alum on days 0, 14, and 28. p value symbols: * represents individual experimental groups compared to the control. *, $p \leq 0.05$, and ***, $p \leq 0.001$, using two-tailed unpaired t tests with Welch's correction (A and B). Data are presented as mean ± SEM.

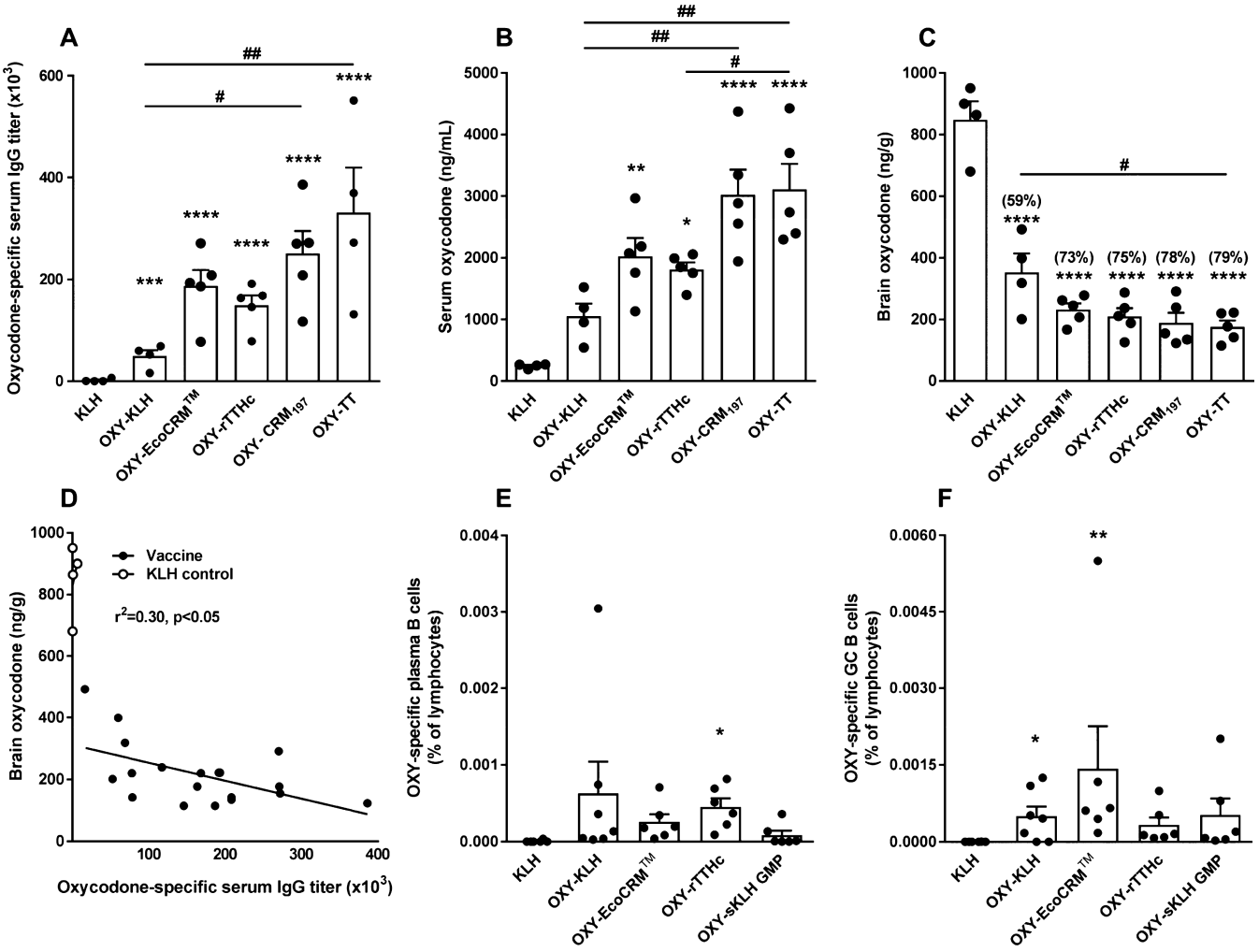

Figure 3.

Vaccines formulated with different carrier proteins show equivalent efficacy against oxycodone and expansion of early hapten-specific B cell subsets. BALB/c mice ($n \geq 4$/group) were sc immunized with unconjugated KLH, OXY-KLH, OXY-EcoCRM, OXY-rTTHc, OXY-CRM_{197}, or OXY-TT, adsorbed on alum adjuvant. (A) Oxycodone-specific serum IgG titers. (B) Serum and (C) brain concentrations of oxycodone after administration of 2.25 mg/kg oxycodone. (D) Oxycodone-specific serum IgG titers vs brain oxycodone concentration (from individual data in panels A and C). BALB/c mice ($n \geq 4$/group) were IM immunized with unconjugated KLH, OXY-KLH, OXY-EcoCRM, OXY-rTTHc, or OXY-sKLH (GMP-grade subunit KLH), formulated with alum. At 7 days post-immunization, B cell lymphocytes from the spleen and lymph nodes were analyzed by flow cytometry. OXY-specific B cells are expressed as percentage (%) of the total lymphocyte population after magnetic enrichment. Shown are OXY-specific B cell subsets: (E) antibody-secreting plasma B cells and (F) germinal center (GC) B cells. *p* value symbols: * represents experimental groups compared to the KLH-only negative control, and # represents interexperimental group comparisons. * or #, $p \leq 0.05$, ** or ##, $p \leq 0.01$, ***, $p \leq 0.001$, and ****, $p \leq 0.0001$, by a log transformed (A), one-way ANOVA paired with Tukey's multiple

comparison test (A, B, C), linear regression (D), and a log transformed, two-tailed unpaired *t* tests with Welch's correction (E, F). Line and error bars represent mean ± SEM.

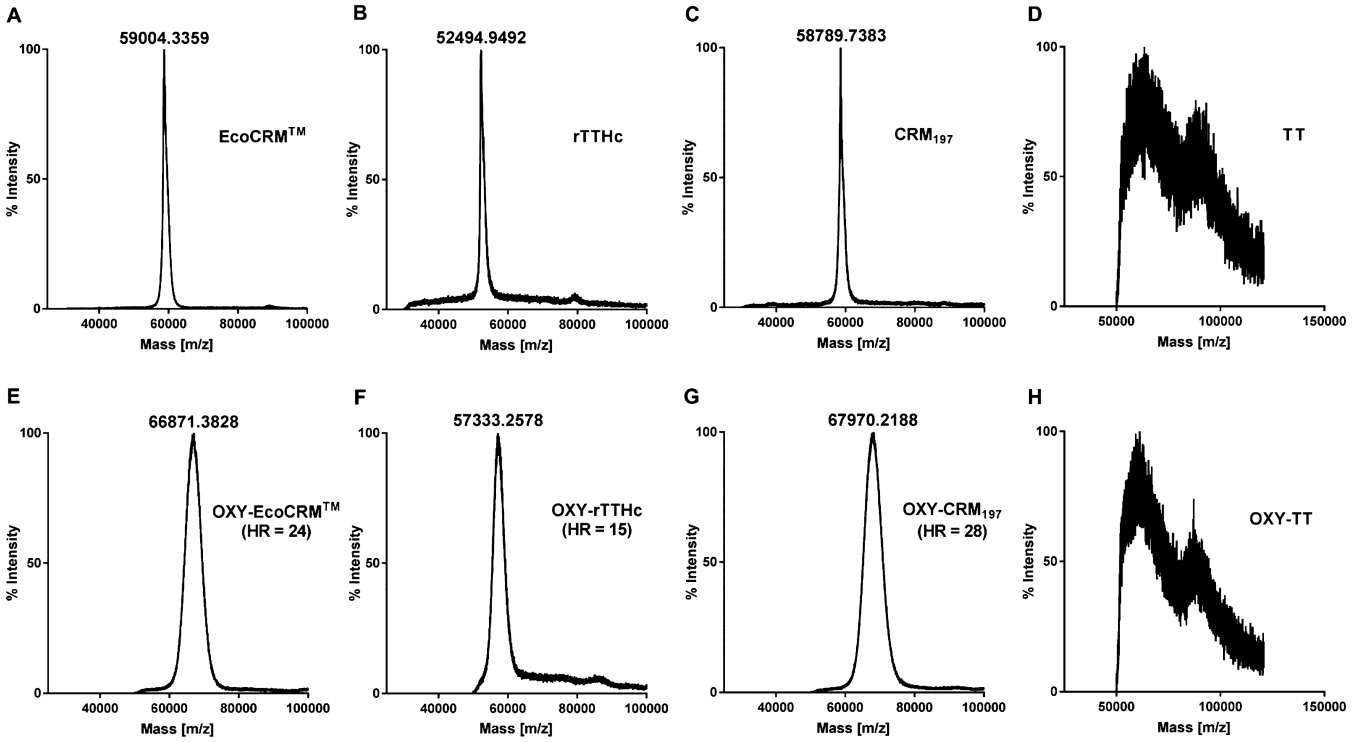

Figure 4.

Characterization of carrier protein and conjugates by MALDI-TOF. The EcoCRM, rTTHc, CRM_{197}, and TT carrier proteins were analyzed before and after conjugation to the $OXY(Gly)_4$ hapten. Upper panels (A, B, C, and D) show carrier proteins prior to conjugation, and lower panels (E, F, G, and H) show results after conjugation. Haptenation ratio (HR) was calculated as follows: $(MW_{OXY(Gly)4–rTTHc} - MW_{rTTHc})/MW_{OXY(Gly)4}$. Samples were analyzed using an Applied Biosystems/MDS SCIEX 54800 MALDI TOF/TOF analyzer operated in high-mass linear mode.

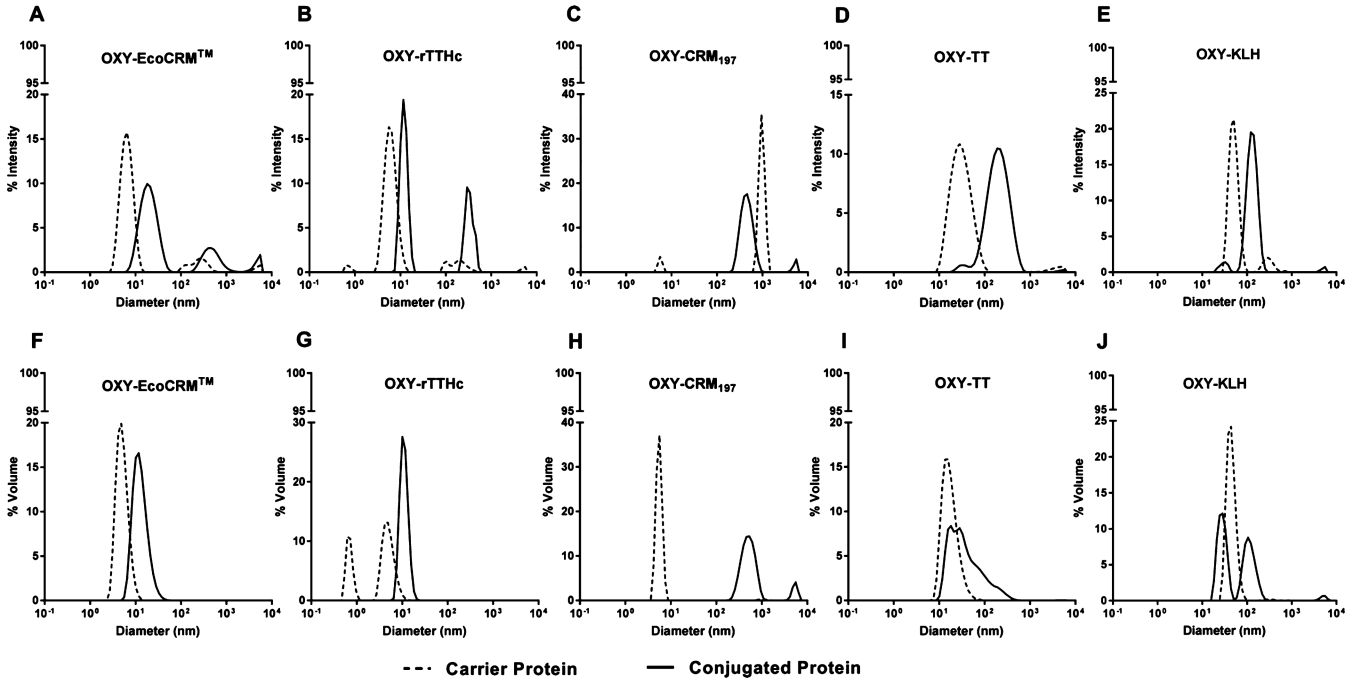

Figure 5.

Characterization of carrier proteins and conjugates by DLS. The carrier protein (75 μL) was assessed before and after conjugation. The percent intensity of (A) EcoCRM, (B) rTTHc, (C) CRM_{197}, (D) TT, (E) native KLH, and their respective OXY-containing conjugates are shown. Panels F–J show the percent volume of each carrier protein and their respective conjugates. Dashed lines represent the carrier protein alone. Solid lines represent the carrier proteins conjugated to the $OXY(Gly)_4$ hapten. The *Z* average [particle diameter (*d*) in nm] is expressed as a decadic logarithm. Data were analyzed with a 633 nm laser under an 173-degree backscatter.

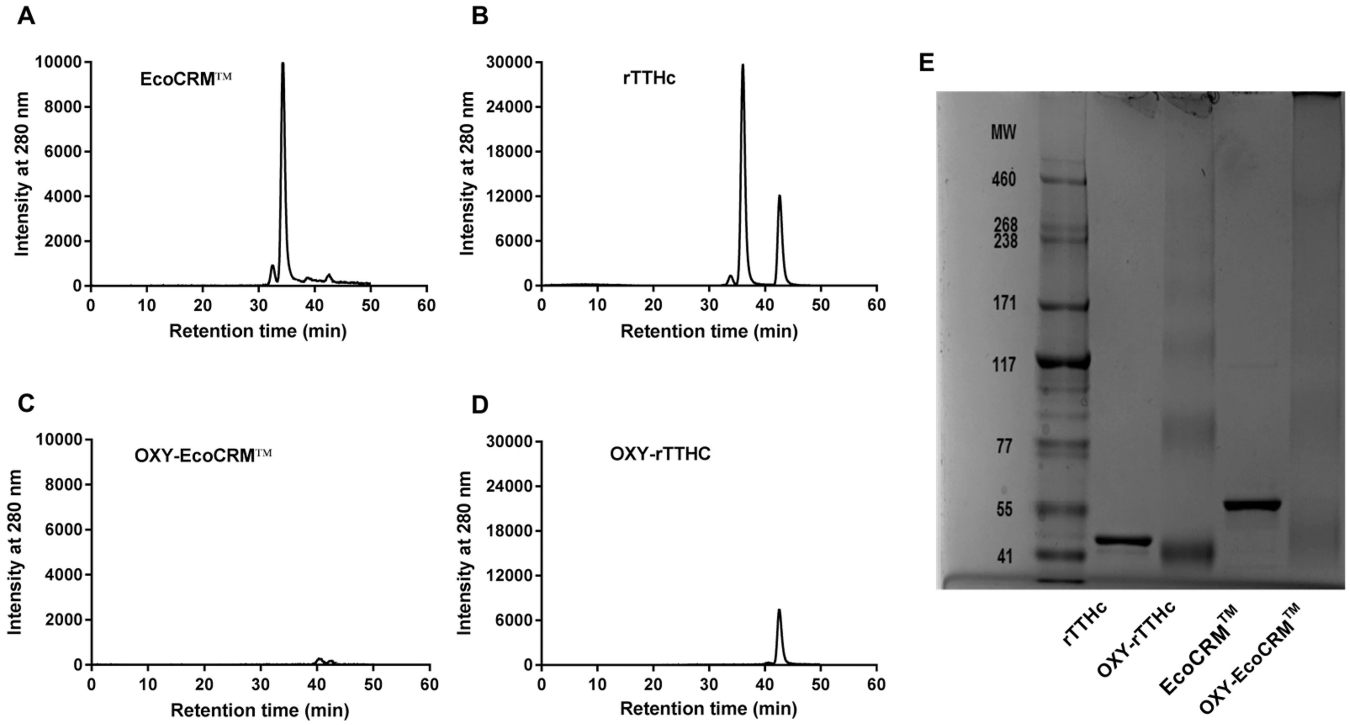

Figure 6.

Characterization of carrier proteins and conjugates by SEC-HPLC and SDS-PAGE. Size exclusion chromatography analysis performed on (A) EcoCRM (62.3 kDa), (B) rTTHc (38.8 kDa), (C) OXY-EcoCRM, and (D) OXY-rTTHc. (E) Image of precast 3–8% polyacrylamide gel. From left to right, in the order of molecular weight reference markers, rTTHc, OXY-rTTHc, EcoCRM, and OXY-EcoCRM.

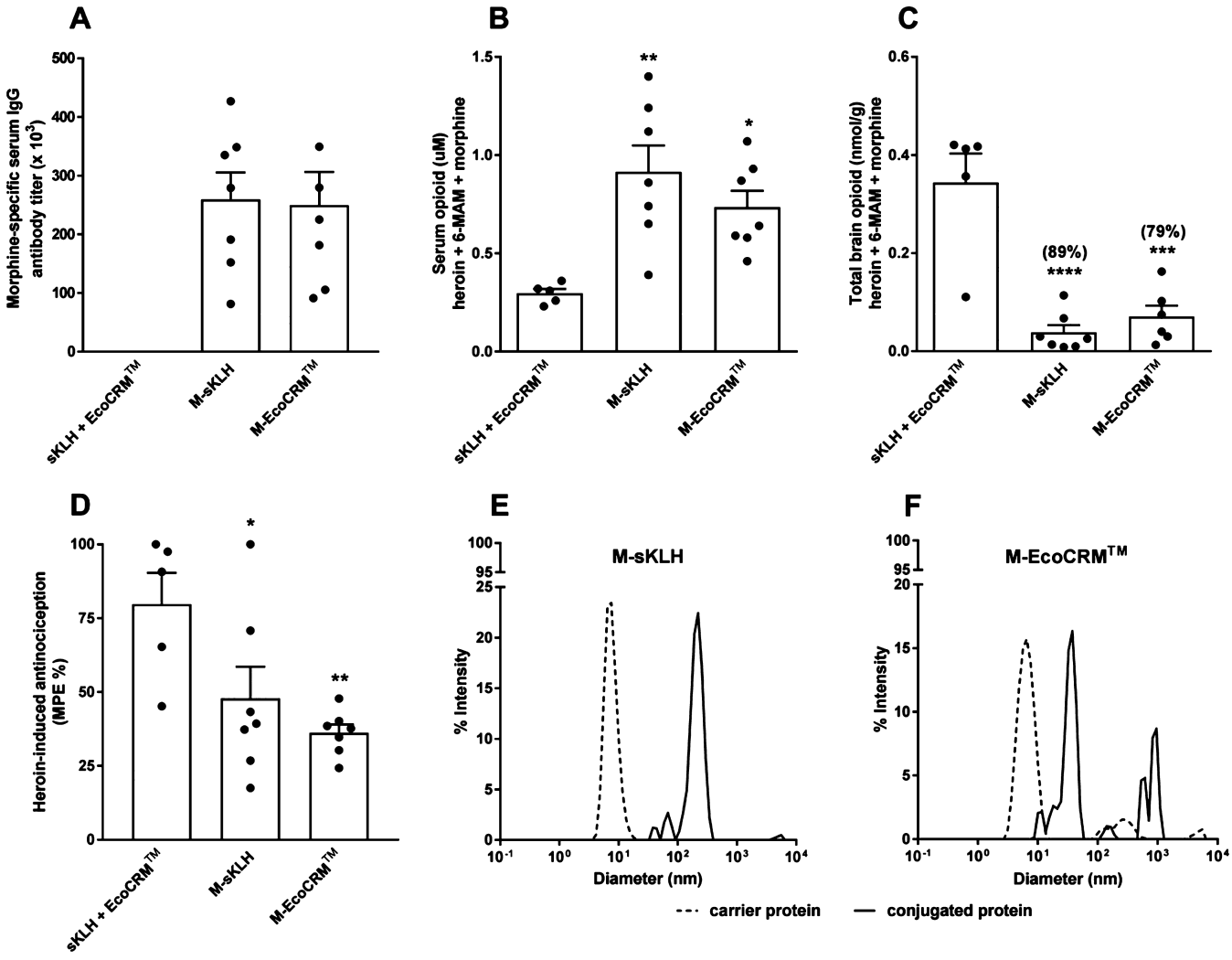

Figure 7.

In vivo and in vitro characterization of heroin vaccines containing different carriers. BALB/c mice ($n \geq 5$/group) were IM immunized with either unconjugated sKLH plus EcoCRM (control), M-sKLH, or M-EcoCRM adsorbed on alum on days 0, 14, and 28. (A) Morphine-specific serum IgG antibody titers. At 30 min after a 1 mg/kg heroin challenge, cumulative concentration of heroin, 6-AM, and morphine in (B) serum and (C) brain. (D) Heroin-induced antinociception in the hot plate assay. Data are mean ± SEM. Statistical symbols: * represents experimental groups compared to the negative control (sKLH+EcoCRM). *, $p \leq 0.05$, **, $p \leq 0.01$, ***, $p \leq 0.001$, and ****, $p \leq 0.0001$ using one-way ANOVA with Tukey's multiple comparison test. DLS characterization of (E) M-sKLH and (F) M-EcoCRM. Dashed lines represent the unconjugated carrier protein, and solid lines represent the heroin conjugate vaccines. The *Z* average [particle diameter (*d*) in nm] is expressed as log base 10. Data were analyzed with a 633 nm laser under a 173-degree backscatter.

Table 1.

Analytical Assays To Characterize Carrier Proteins and Oxycodone Conjugate Vaccines[a]

Test compound	MALDI-TOF	DLS	SEC-HPLC	SDS PAGE	MW (kDa)	HR
KLH	X	√	X	N/A		
OXY-KLH	X	√	X	N/A		
rTTHc	√	√	X	√	52.5	
OXY-rTTHc	√	√	X	X	57.3	15
EcoCRM	√	√	X	√	59.0	
OXY-EcoCRM	√	√	X	X	66.9	24
TT	X	√	N/A	N/A		
OXY-TT	X	√	N/A	N/A		
CRM_{197}	√	√	N/A	N/A	58.8	
OXY-CRM_{197}	√	X	N/A	N/A	68.0	28

[a]When possible, unconjugated and conjugated proteins were characterized with MALDI-TOF, DLS, SEC-HPLC, and SDS PAGE. The table reports the haptenation ratio (HR) according to the molecular weight (MW) as measured by MALDI-TOF.